LETTERS

Glaciation as a destructive and constructive control on mountain building

Stuart N. Thomson[1,2], Mark T. Brandon[2], Jonathan H. Tomkin[4], Peter W. Reiners[1], Cristián Vásquez[3] & Nathaniel J. Wilson[2]

Theoretical analysis predicts that enhanced erosion related to late Cenozoic global cooling can act as a first-order influence on the internal dynamics of mountain building, leading to a reduction in orogen width and height[1–3]. The strongest response is predicted in orogens dominated by highly efficient alpine glacial erosion, producing a characteristic pattern of enhanced erosion on the windward flank of the orogen and maximum elevation controlled by glacier equilibrium line altitude[3,4], where long-term glacier mass gain equals mass loss. However, acquiring definitive field evidence of an active tectonic response to global climate cooling has been elusive[5]. Here we present an extensive new low-temperature thermochronologic data set from the Patagonian Andes, a high-latitude active orogen with a well-documented late Cenozoic tectonic, climatic and glacial history. Data from 38° S to 49° S record a marked acceleration in erosion 7 to 5 Myr ago coeval with the onset of major Patagonian glaciation[6] and retreat of deformation from the easternmost thrust front[7]. The highest rates and magnitudes of erosion are restricted to the glacial equilibrium line altitude on the windward western flank of the orogen, as predicted in models of glaciated critical taper orogens where erosion rate is a function of ice sliding velocity[3,8]. In contrast, towards higher latitudes (49° S to 56° S) a transition to older bedrock cooling ages signifies much reduced late Cenozoic erosion despite dominantly glacial conditions here since the latest Miocene[6]. The increased height of the orogenic divide at these latitudes (well above the equilibrium line altitude) leads us to conclude that the southernmost Patagonian Andes represent the first recognized example of regional glacial protection of an active orogen from erosion, leading to constructive growth in orogen height and width.

The excellent match between non-volcanic summit elevations and southward decrease in perennial snowline in the southern Andes is cited as a classic example of first-order climatic control on mountain topography[9–11]. According to the glacial 'buzzsaw' hypothesis, highly efficient alpine glacial erosion limits the development of topography above the glacial equilibrium line altitude (ELA)[13]. Supporting this hypothesis, in the northern Patagonian Andes the match between elevation and snowline is maintained despite widely variable late Cenozoic rock uplift rates[12]. However, south of about 45° S, this relationship breaks down[14], with the summits and mean elevation of the orogenic divide situated well above the long-term mean ELA, in conflict with the idea of a global glacial buzzsaw[11,13].

A strong link between glaciation and reduction in topographic relief is a key component of recent models that demonstrate that enhanced erosion associated with late Cenozoic climate change can alter the internal dynamics of active mountain belts[1,3,15]. These models call into question earlier claims that climatically enhanced late Cenozoic erosion rates and isostatic rebound increased relief and summit elevations, inducing a positive feedback of more erosion and rock uplift, and the illusion of increased tectonic activity[16]. Demonstrating the validity of these model-based arguments using field observations is complicated by complex real-world interactions between climate change, erosion and tectonics[5]. Increased rock uplift, erosion, and sediment supply in response to climate change alone is insufficient to distinguish between an active tectonic or passive isostatic response to climate change. True diagnosis requires that such increases are accompanied by a reduction in the height and width of a critical-taper orogen, with deformation retreating to the core of the range[5].

We chose to test these concepts by applying low-temperature thermochronometry to evaluate spatial and temporal patterns of erosion in the glaciated Patagonian Andes, including higher latitudes where the match between elevation and snowline breaks down. Glaciated orogens are theoretically more responsive to changes in climate and tectonics than fluvially dominated orogens[3], making any response more readily detectable. Widespread mountain glaciation in Patagonia began sometime between 7 and 5 Myr ago (ref. 6), providing a much longer record than comparable Northern Hemisphere orogens[4]. This time span is similar to typical predicted response times of glaciated orogens to changes in climate and tectonics of 1.5 to 5.5 Myr (ref. 3).

We report 246 new apatite (U–Th)/He ages and 136 new apatite fission-track (AFT) ages from 146 samples collected along the length and breadth of the Patagonian Andes from 38° S to 56° S, as well as 165 previously published AFT ages (Fig. 1, Supplementary Note 2 and Supplementary Tables 1–3). All ages less than about 10 Myr that are relevant to our interpretations are considerably younger than the stratigraphic or magmatic crystallization age of the rocks and reflect the time of cooling related to removal of overburden by erosion.

Apatite (U–Th)/He and AFT age–elevation relationships from close to the main divide in the more northerly parts of the Patagonian Andes (Fig. 2) demonstrate a marked change from older (high elevation) to younger (low elevation) ages, indicative of an acceleration of erosion rates[17] at about 7 Myr ago. The timing of this acceleration is well after the onset of initial surface uplift of the Patagonian Andes, dated to around 17–14 Myr ago[18], but is remarkably similar to the onset of widespread glaciation in the region[6], supporting the previously recognized strong erosional response of the orogen at these latitudes to cooler climate and the onset of erosive alpine glaciation[12]. More importantly, a diagnostic active tectonic response to climatic cooling is implied by contemporaneous cessation of faulting at the easternmost thrust front at similar latitudes between 9 and 6 Myr ago[7,12], with shortening confined to more internal parts of the orogen, recorded locally by a transition from strike-slip motion to transpressional uplift along the Liquiñe–Ofqui fault since ~7 Myr ago[12].

[1]Department of Geosciences, University of Arizona, Tucson, Arizona 85271, USA. [2]Department of Geology and Geophysics, Yale University, New Haven, Connecticut 06511, USA. [3]Departamento de Geología, Universidad de Chile, Casilla 13518, Correo 21, Santiago, Chile. [4]Department of Geology, University of Illinois, Urbana, Illinois 61801, USA.

©2010 Macmillan Publishers Limited. All rights reserved

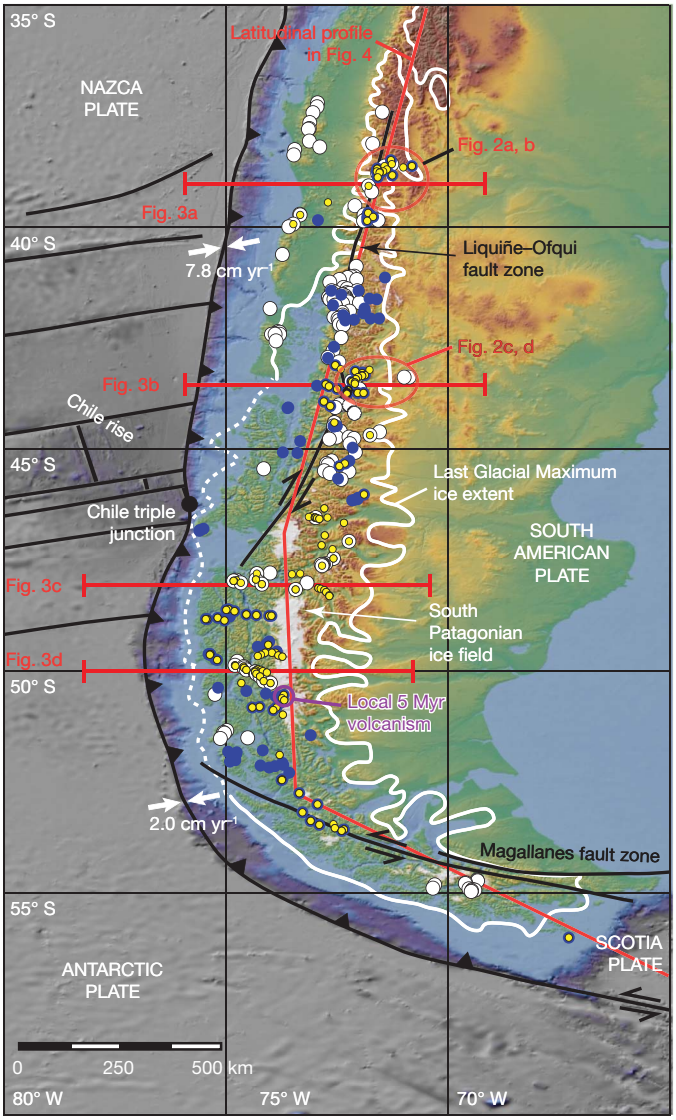

Figure 1 | Topographic and tectonic map of southernmost South America showing sample locations. Apatite (U–Th)/He locations are shown as small yellow circles; AFT locations are shown as medium blue circles. Also included are the locations of samples used to plot age–elevation relationships in Fig. 2, the positions of the transects shown in Fig. 3, and the latitudinal profile in Fig. 4 (all marked in red). Details on previously published apatite fission-track samples (large white circles), digital elevation data, location of Last Glacial Maximum ice extent (delimited by white line), volcanic ages (purple circle), and plate convergence velocities (white arrow pairs) are given in Supplementary Notes 1 and 2, and Supplementary Table 3.

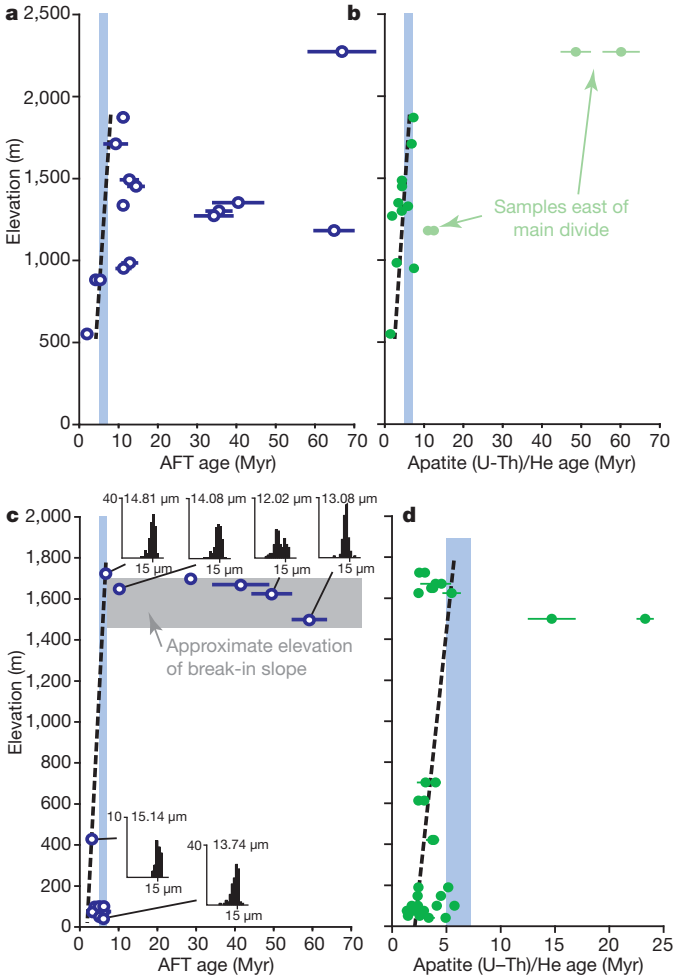

Figure 2 | Age–elevation relationships from two high-relief transects. The reference slope is 0.5 mm yr^{-1} (black dashed line in all panels). The onset of glaciation is 5–7 Myr ago (thick blue line in all panels). **a**, AFT age–elevation relationship (AER) from 38–40° S. **b**, Apatite (U–Th)/He AER from the same samples, showing younger ages at lower elevations, indicative of the onset of enhanced erosion ~7 Myr ago coeval with the onset of major glaciation in southern South America. **c**, AFT AER from 43–44° S showing a similar transition to younger ages with longer mean-track-length distributions (histograms for the indicated data points show mean track length versus number of fission tracks) at lower elevations ~7 Myr ago. The break-in slope[17] approximates the former closure depth of the thermochronometric system (~4.1 km for AFT for erosion rates of ~0.5 mm yr^{-1}; ref. 30) immediately before accelerated erosion ~7 Myr ago. This equates to a time-averaged erosion rate of ~0.6 mm yr^{-1} since then. The samples close to sea level represent an additional 1.5 km of erosion (total of 5.6 km erosion) requiring a time-averaged erosion rate of 0.8 mm yr^{-1} since 7 Myr ago. **d**, Apatite (U–Th)/He ages from the same samples show a similar AER. All age error bars that are larger than the symbol are 1 sigma.

The spatial patterns of both AFT and apatite (U–Th)/He ages across three transects north of 49° S (Fig. 3a–c) reveal a distinct U-shaped pattern, with the age minima (<5 Myr)—and hence the highest magnitude and rates of erosion—concentrated where the ELA intersects the topography on the windward western flank of the orogen. This pattern matches the predictions of numeric and analytic models of the expected erosional response to increased alpine glaciation in critical taper orogens[3,8], and is a characteristic feature of the windward flank of other high-latitude orogens dominated by temperate alpine glaciation[4,19]. In such orogens an additional link between precipitation rate and thermochronometric age minima has been recognized[19]. A natural coupling between maximum erosion rates, precipitation rates, and the intersection of ELA with topography is to be expected, because enhanced precipitation in the form of snowfall on the windward flank results in thicker ice close to the ELA, with resultant increased sliding velocity and basal shear stress leading to higher localized erosion rates. Further support for glacially enhanced erosion, rather than the location of local active structures, as a control on the observed age patterns across these three northernmost transects is provided by the presence of an age minimum close to the ELA on the windward flank in the absence of any arc-parallel faulting between 47–49° S (Fig. 3c). The observed correlation between timing of onset of glaciation, deformation front retreat, and concentration of deformation and acceleration of erosion rates within the orogen interior supports the idea of the Patagonian Andes north of ~47–49° S as being one of the most convincing examples worldwide of the destructive active tectonic response of an orogen (through its reduction in width and height) to climate change and the onset of glaciation.

©2010 Macmillan Publishers Limited. All rights reserved

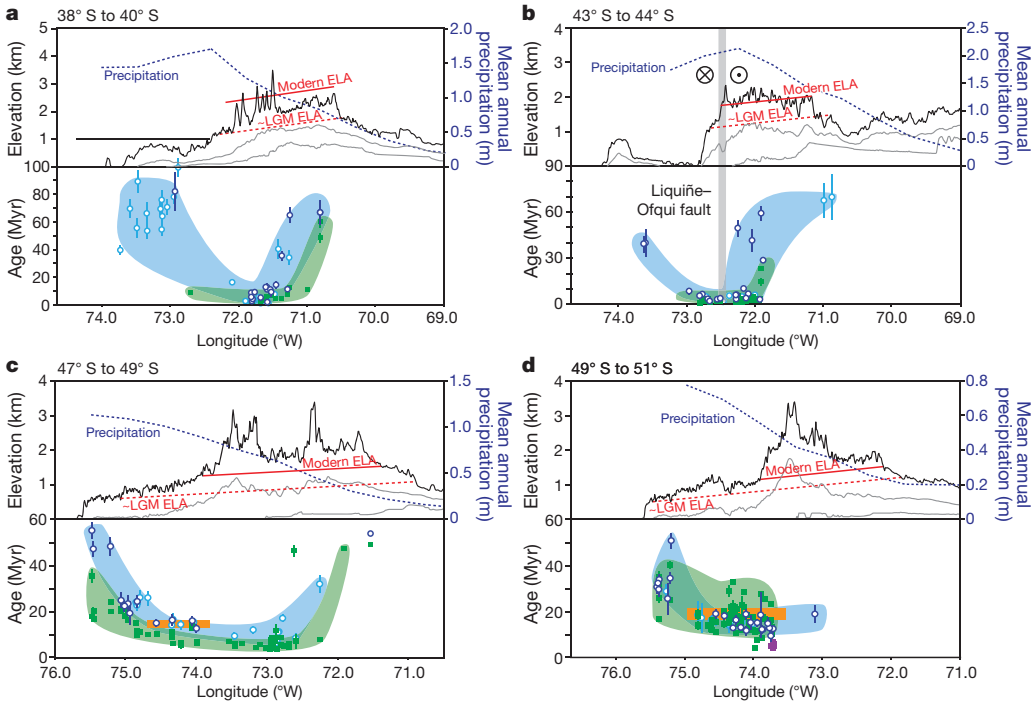

Figure 3 | Four east–west transects across the Patagonian Andes at different latitudes. New apatite (U–Th)/He ages are shown as green circles, new AFT ages as dark blue circles, and the previously published AFT ages as light blue circles; 1 sigma error bars. **a**–**c**, The three northernmost transects show a distinct U-shaped age minimum for both thermochronometers (less than about 5 Myr ago) on the windward (enhanced precipitation) side of the range whereas the profile furthest south (**d**) shows no such relationship, despite the presence of widespread fiords and ongoing glaciation. Transects include age data, mean, maximum, and minimum elevation information from a 1° swath (**a**, **c**, **d**) or 0.5° swath (**b**) either side of each transect. The ELA is from refs 9 and 14. The mean annual precipitation data are from the UNEP/GRID database (http://www.grid.unep.ch/). The highlighted region of Miocene (about 20 Myr ago) magmatism (orange) places an upper age limit on most of the samples from this part of the transect.

In contrast, the more southerly transect at 49–51° S (Fig. 3d) shows exclusively old apatite (U–Th)/He and AFT ages >10 Myr (with the exception of several local ~5-Myr-old volcanic rocks), which implies inefficient regional glacial erosion at these latitudes over the last ~10 Myr. A southward increase in the youngest age (and hence a decrease in long-term glacial erosion efficiency) across the whole orogen can be seen clearly in latitudinal swath profiles (Fig. 4). For both systems this transition occurs between about 45° S and 50° S, being more apparent in the fission-track data. Importantly, this transition coincides in latitude with an increase in the non-volcanic maximum and mean elevation of the main divide south of ~45° S to well above the Last Glacial Maximum and the modern ELA, demonstrating that the southernmost Patagonian Andes do not support the glacial buzzsaw hypothesis[11]. A regional decrease in erosional efficiency at these latitudes is supported by a southward decrease in the amount of glacial-marine fjord sedimentation from thick temperate glacial facies north of 46° S, to thinner transitional polar glacial facies at ~54° S (ref. 20), as well as by the preservation of 5-Myr-old dacite lava flows forming islands in a fjord at 50° S (ref. 21).

The remarkable latitudinal coincidence between lower glacial erosion efficiency and higher elevations of the southern Patagonian Andes is consistent with glaciation having acted effectively at a regional orogenic scale to protect the landscape from erosion over much of the latest Cenozoic era. In critical-taper orogens, if there is no change in accretionary flux, a decrease in erosional efficiency (and hence reduced erosional efflux) is predicted to act in a constructive manner, leading to an increase in wedge width and height[5,15]. The assumption of no change in accretionary flux in the Patagonian Andes is corroborated by at least 10 Myr of steady subduction of the Antarctic plate south of ~48°S (ref. 7). Furthermore, if the approximately 1,000 m higher elevation of the divide at these latitudes were the result of surface uplift owing to the lack of significant erosion since the onset of widespread glaciation ~7 to 5 Myr ago, this would require time-averaged tectonic and surface uplift rates of ~0.14 to 0.2 mm yr^{-1}. These rates match remarkably well with post-early Miocene surface uplift rates of 0.07 to 0.22 mm yr^{-1} estimated from 1,900 m elevation transitional marine facies rocks at 47° S (ref. 22). Evidence for increasing wedge width is implied by active reverse fault scarps and tilting of Pliocene basalts at the eastern mountain front at 49° 30′ S (ref. 23), as well as by coeval (6 to 5 Myr ago) uplift and denudation[24] and late Cenozoic eastward-migrating deep-seated thrusts[25] on the eastern side of the orogen at 51° S.

The lack of regionally extensive erosion south of about 45° S implies that any glacier basal flow (and hence erosive potential) must have been very spatially restricted. This agrees with a coupled ice-sheet/climate numeric model of the Patagonian icesheet[26], in which during the Last Glacial Maximum high ice-flow velocities are limited to relatively widely spaced, very narrow ice-streams at the margins of the ice sheet, surrounded by extensive areas of very-low-velocity ice. The predominance of highly resistant granitic bedrock and complex geologically controlled fjord geometry south of about 45° S probably further acted to confine regions of fast-flowing ice, as well as limit basal ice flow, as has been proposed to explain limited erosion in the tectonically inactive East Greenland fjord region[27] (see Supplementary Note 3 for additional discussion).

Previously, glacial preservation of landscape has only been documented beneath ice sheets and ice caps in tectonically passive polar continental settings[28,29]. Consequently, the southernmost Patagonian Andes represent the first demonstrable example of regional glacial protection of an active orogen resulting in a constructive tectonic response to late Cenozoic climate cooling. That glaciation can act to protect an active orogen from erosion opens up the intriguing possibility that, given favourable glacio-climatic, geologic and tectonic conditions, a cooling climate can act to enhance topographic relief, not in the manner originally envisaged in ref. 16 through passive isostatic response to locally enhanced erosion, but by inhibiting erosion to promote further accretionary growth in orogen height and width.

©2010 Macmillan Publishers Limited. All rights reserved

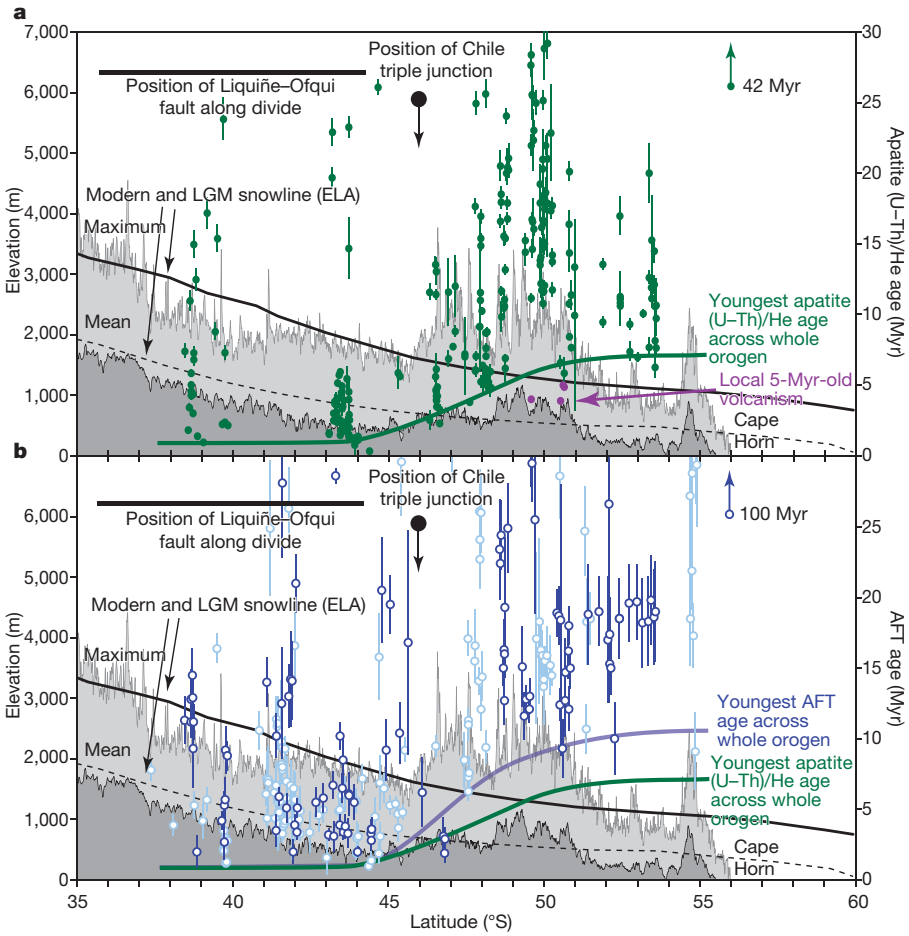

Figure 4 | Latitudinal swath profiles showing apatite (U–Th)/He and AFT ages. Also plotted are maximum and mean elevation (from a 4° east–west swath centred along the profile in Fig. 1), as well as the modern and mean glacial ELA[14]. **a**, Apatite (U–Th)/He ages (green circles); **b**, AFT ages (new AFT ages are shown as dark blue circles and the previously published AFT ages as light blue circles). All age error bars are 1 sigma. We note that with the exception of some ages from independently dated Pliocene (5-Myr-old) dacite at about 50° S (ref. 21), the minimum apatite (U–Th)/He and AFT ages both show a distinct increase south of about 45° S, implying a significant decrease in total amounts and rates of post-10-Myr-ago erosion at these latitudes, despite dominantly glacial conditions here since ~7 Myr ago.

METHODS SUMMARY

(U–Th)/He dating was performed on handpicked apatite grains measured for alpha-ejection correction following methods in ref. 19. Single or multiple crystals were loaded into 1 mm Pt tubes, and degassed by heating with a Nd-YAG laser. The concentration of ^{4}He was determined by ^{3}He isotope dilution and a quadrupole mass spectrometer. U, Th and Sm concentrations were obtained by isotope dilution using an inductively coupled plasma mass spectrometer. Alpha-ejection correction was applied to derive a corrected (U–Th)/He age. Fission track dating was done following the methods in ref. 12. CN5 and IRMM540R glass was used to monitor neutron fluence during irradiation at the Oregon State University Triga Reactor, Corvallis, USA. Zeta calibration factors of 342.5 ± 3.8 (CN5 apatite), and 352.4 ± 12.1 (IRMM540R apatite) were used in the calculation of central ages.

Received 9 March; accepted 15 July 2010.

1. Whipple, K. X. & Meade, B. J. Orogen response to changes in climatic and tectonic forcing. *Earth Planet. Sci. Lett.* **243**, 218–228 (2006).
2. Stolar, D., Roe, G. & Willett, S. Controls on the patterns of topography and erosion rate in a critical orogen. *J. Geophys. Res.* **112**, F04002, doi: 10.1029/2006JF000713 (2007).
3. Tomkin, J. H. & Roe, G. H. Climate and tectonic controls on glaciated critical-taper orogens. *Earth Planet. Sci. Lett.* **262**, 385–397 (2007).
4. Berger, A. L. *et al.* Quaternary tectonic response to intensified glacial erosion in an orogenic wedge. *Nature Geosci.* **1**, 793–799 (2008).
5. Whipple, K. X. The influence of climate on the tectonic evolution of mountain belts. *Nature Geosci.* **2**, 97–104 (2009).
6. Mercer, J. H. & Sutter, J. F. Late Miocene earliest Pliocene glaciation in southern Argentina—implications for global icesheet history. *Palaeogeogr. Palaeoclimatol. Palaeoecol.* **38**, 185–206 (1982).
7. Ramos, V. A. Seismic ridge subduction and topography: foreland deformation in the Patagonian Andes. *Tectonophysics* **399**, 73–86 (2005).
8. Tomkin, J. H. Coupling glacial erosion and tectonics at active orogens: a numerical modeling study. *J. Geophys. Res.* **112**, F02015, doi: 10.1029/2005JF000332 (2007).
9. Porter, S. C. Pleistocene glaciation in the southern Lake District of Chile. *Quat. Res.* **16**, 263–292 (1981).
10. Montgomery, D. R., Balco, G. & Willett, S. D. Climate, tectonics, and the morphology of the Andes. *Geology* **29**, 579–582 (2001).
11. Egholm, D. L., Nielsen, S. B., Pedersen, V. K. & Leseman, J.-E. Glacial effects limiting mountain height. *Nature* **460**, 884–888 (2009).
12. Thomson, S. N. Late Cenozoic geomorphic and tectonic evolution of the Patagonian Andes between latitudes 42°S and 46°S: an appraisal based on fission-track results from the transpressional intra-arc Liquine-Ofqui fault zone. *Geol. Soc. Am. Bull.* **114**, 1159–1173 (2002).
13. Brozovic, N., Burbank, D. W. & Meigs, A. J. Climatic limits on landscape development in the northwestern Himalaya. *Science* **276**, 571–574 (1997).
14. Broecker, W. S. & Denton, G. H. The role of ocean-atmosphere reorganizations in glacial cycles. *Quat. Sci. Rev.* **9**, 305–341 (1990).
15. Willett, S. D. Orogeny and orography: the effects of erosion on the structure of mountain belts. *J. Geophys. Res.* **104**, 28957–28981 (1999).
16. Molnar, P. & England, P. Late Cenozoic uplift of mountain ranges and global climate change—chicken or egg? *Nature* **346**, 29–34 (1990).
17. Fitzgerald, P. G., Sorkhabi, R. B., Redfield, T. F. & Stump, E. Uplift and denudation of the central Alaska Range: a case study in the use of apatite fission track thermochronology to determine absolute uplift parameters. *J. Geophys. Res.* **100**, 20175–20191 (1995).
18. Blisniuk, P. M., Stern, L. A., Chamberlain, C. P., Idleman, B. & Zeitler, P. K. Climatic and ecologic changes during Miocene surface uplift in the southern Patagonian Andes. *Earth Planet. Sci. Lett.* **230**, 125–142 (2005).
19. Reiners, P. W., Ehlers, T. A., Mitchell, S. G. & Montgomery, D. R. Coupled spatial variations in precipitation and long-term erosion rates across the Washington Cascades. *Nature* **426**, 645–647 (2003).
20. DaSilva, J. L., Anderson, J. B. & Stravers, J. Seismic facies changes along a nearly continuous 24 degrees latitudinal transect: the fjords of Chile and the northern Antarctic peninsula. *Mar. Geol.* **143**, 103–123 (1997).

©2010 Macmillan Publishers Limited. All rights reserved

21. Hervé, F., Pankhurst, R. J., Fanning, C. M., Calderón, M. & Yaxley, G. M. The South Patagonian batholith: 150 my of granite magmatism on a plate margin. *Lithos* **97,** 373–394 (2007).
22. Flynn, J. J. *et al.* A new fossil mammal assemblage from the southern Chilean Andes: implications for geology, geochronology, and tectonics. *J. S. Am. Earth Sci.* **15,** 285–302 (2002).
23. Coutand, I. *et al.* Structure and kinematics of a foothills transect, Lago Viedma, southern Andes (49 degrees 30′ S). *J. S. Am. Earth Sci.* **12,** 1–15 (1999).
24. Fosdick, J. C. Late Miocene exhumation of the Magallanes Basin and sub-Andean fold belt, southern Chile: new constraints from apatite U-Th/He thermochronology. *GSA Abstr.* **39,** 341 (2007).
25. Harambour, S. M. Deep-seated thrusts in the frontal part of the Magallanes fold and thrust belt, Ultima Esperanza, Chile. *15th Congr. Geol. Argentino Actas* **3,** 232 (2002).
26. Hulton, N. R. J., Purves, R. S., McCulloch, R. D., Sugden, D. E. & Bentley, M. J. The Last Glacial Maximum and deglaciation in southern South America. *Quat. Sci. Rev.* **21,** 233–241 (2002).
27. Swift, D. A., Persano, C., Stuart, F. M., Gallagher, K. & Whitham, A. A reassessment of the role of ice sheet glaciation in the long-term evolution of the East Greenland fjord region. *Geomorphology* **97,** 109–125 (2008).
28. Sugden, D. E. Glacial erosion by the Laurentide ice sheet. *J. Glaciol.* **20,** 367–391 (1978).
29. Fabel, D. *et al.* Landscape preservation under Fennoscandian ice sheets determined from in situ produced Be-10 and Al-26. *Earth Planet. Sci. Lett.* **201,** 397–406 (2002).
30. Reiners, P. W. & Brandon, M. T. Using thermochronology to understand orogenic erosion. *Annu. Rev. Earth Planet. Sci.* **34,** 19–66 (2006).

Supplementary information is linked to the online version of this paper at www.nature.com/nature.

Acknowledgements This work was supported by the NSF Geomorphology and Land Use Dynamics and Tectonics Award EAR0447140. S. Nicolescu assisted with (U–Th)/He analysis. S.N.T. thanks F. Hervé for numerous invitations to take part in boat expeditions in the Chilean fjords made possible through Chilean Fondecyt awards 1010412, 1050431, 7010412 and 7060240. Captains C. Alvarez Senior and Junior, V. Alvarez, D. Lleufo and C. Porter expertly guided us through the Chilean fjords on the boats *Mama Dina*, *Penguin*, *Foam*, *21 de Mayo* and R/V *Gondwana*. We thank R. Fuenzalida and C. Mpodozis at ENAP/Sipetrol for allowing us to publish the apatite fission track data from the SP samples. H. Echtler and J. Glodny at the GFZ Potsdam, and F. Hervé at the Universidad de Chile provided additional apatite sample separates. This work benefited from discussions with G. Roe and M. Kaplan.

Author Contributions Writing and interpretation was done by S.N.T. with contributions from M.T.B., J.H.T. and P.W.R. Fieldwork was performed by S.N.T., M.T.B., J.H.T., P.W.R. and C.V. Apatite fission track analysis was done by S.N.T. (U–Th)/He dating was carried out by S.N.T., N.J.W. and C.V.

Author Information Reprints and permissions information is available at www.nature.com/reprints. The authors declare no competing financial interests. Readers are welcome to comment on the online version of this article at www.nature.com/nature. Correspondence and requests for materials should be addressed to S.N.T. (thomson@email.arizona.edu).

©2010 Macmillan Publishers Limited. All rights reserved

Note 1:
In Figure 1, the digital elevation data was obtained from the SRTM 30 Plus data set (Becker et al., 2009). The outline of the modern glaciers and ice field was obtained from the GLIMS glacier database (http://glims.colorado.edu/glacierdata/). Last Glacial Maximum ice extent (shown in grey) is from Singer et al. (2004) after Caldenius (1932) and Clapperton (1993). Local 5 Ma aged volcanism (Hervé et al., 2007) (outlined in purple) resulted in several anomalously young AFT and AHe ages obtained from these rocks and reset ages in older bedrock with 10 km of this volcanism. The very presence of dacite lava flows of this age means that nearby similarly young ages cannot reflect cooling related to erosion. Plate convergence velocities and vectors after Cande & Leslie (1986) and Somoza (1998).

Note 2:
Previously published apatite fission track data (Adriasola et al., 2006; Glodny et al., 2008; Nelson, 1982; Thomson et al., 2001; Thomson, 2002; Thomson & Hervé, 2002 and Willner et al., 2004) were used in the compilation of Figures 1, 3, and 4. All the data used in these figures, as well as the sample locations are presented in Supplementary Table 3.

Note 3:
The low temperature thermochronologic data presented in this study require that regionally averaged total amounts of erosion and hence late Cenozoic erosion rates south of about 45°S were insufficient to be recorded by our broad, high spatial resolution low temperature thermochronometry data set (< 1.5 to 2 km total erosion for the AHe system). Such spatially restricted total erosion (significantly less than 50% of the whole surface area of the orogen south of about 45°S) will lead to a substantial orogen mass flux imbalance (such that the total accretionary flux will greatly exceed the total erosional efflux) requiring growth of the orogen to maintain its critical taper (self similarity of its height to width ratio) as outlined by Whipple and others (Whipple, 2009; Stolar et al., 2007; Tomkin & Roe, 2007).

Additional support for a southward transition to lower glacial erosion efficiency (at the scale of the whole surface area of the orogen) comes from the observation that the modern mean annual temperature at the coast drops below 7°C south of about 48°S (Hulton et al., 2002, after Romero 1985). Given the ca. 6-7°C cooling required by the glacier models of Hulton et al (2002) to replicate the extent of the LGM Patagonian ice sheet, 48°S would have equated to the northern limit of the 0°C mean annual sea-level temperature at this time, especially at higher elevations, such that cold-based conditions would most likely have predominated south of this latitude leading to a widespread reduction in glacial erosion efficiency (with the exception of a few localized and narrow ice streams).

Furthermore, Kaplan et al. (2009) illustrate that the maximum extent of glaciation to the east of the Andes south of ca. 50°S has gradually decreased over the last ca. 1 Ma. They speculate that

this was the result of a gradual decrease in elevation of the main divide owing to enhanced glaciation, in apparent contradiction to our thermochronometric data that demonstrate a reduction in erosion rates at these latitudes. However, the observation of gradually decreasing maximum glacial extent east of the divide with gradual increase in elevation of the divide are easily reconciled by ice sheet model observations (Hulton et al., 2002) where increased elevation of the Patagonian icesheet results in decreased availability of moisture in the eastern rain shadow, leading to decreased snowfall, mass balance, and hence maximum ice extent.

References Used in Supplementary Information

Adriasola, A. C., Thomson, S. N., Brix, M. R., Herve, F. & Stockhert, B. Postmagmatic cooling and late Cenozoic denudation of the North Patagonian Batholith in the Los Lagos region of Chile, 41 degrees-42 degrees 15'S. *Int. J. Earth Sci.* **95**, 504-528 (2006).

Becker, J. J., Sandwell, D.T., Smith, W.H.F., Braud, J., Binder, B., Depner, J., Fabre, D., Factor, J., Ingalls, S., Kim, S.-H., Ladner, R., Marks, K., Nelson, S., Pharaoh, A., Trimmer, R., Von Rosenberg, J., Wallace, G., & Weatherall, P. Global Bathymetry and Elevation Data at 30 Arc Seconds Resolution: SRTM30_PLUS, *Marine Geodesy*, **32**, 355-371 (2009).

Caldenius, C.G. Las glaciaciones Cuaternarias en la Patagonia and Tierra del Fuego. *Geografiska Annaler* **14,** 1-164 (1932).

Cande, S.C. & Leslie, R.B. Late Cenozoic Tectonics of the southern Chile trench. *J. Geophys. Res.* **91**, 471-496 (1986).

Clapperton, C.M. Quaternary geology and geomorphology of South America: New York, Elsevier, 779pp. (1993).

Glodny, J., Grafe, K., Echtler, H. & Rosenau, M. Mesozoic to Quaternary continental margin dynamics in South-Central Chile (36-42 degrees S): the apatite and zircon fission track perspective. *Int. J. Earth Sci.* **97**, 1271-1291, doi: 10.1007/S00531-007-0203-1 (2008).

Hervé, F., Pankhurst, R. J., Fanning, C. M., Calderón, M. & Yaxley, G. M. The South Patagonian batholith: 150 my of granite magmatism on a plate margin. *Lithos* **97**, 373-394 (2007).

Hulton, N. R. J., Purves, R. S., McCulloch, R. D., Sugden, D. E. & Bentley, M. J. The Last Glacial Maximum and deglaciation in southern South America. *Quat. Sci. Rev.* **21**, 233-241 (2002).

Kaplan, M.R., Hein, A.S., Hubbard, A. & Lax, S.M. Can glacial erosion limit the extent of glaciation? *Geomorphology* 103 172-179 (2009).

Nelson, E. P. Post-Tectonic Uplift of the Cordillera Darwin Orogenic Core Complex - Evidence from Fission-Track Geochronology and Closing Temperature Time Relationships. *J. Geol. Soc.* **139**, 755-761 (1982).

Romero H. Geografia de Chile: Geografia de los Climas. Instituto Geografico Militar, Santiago. (1985).

Singer, B.S., Ackert, R.P. & Guillou, H. $^{40}Ar/^{39}Ar$ and K-Ar chronology of Pleistocene glaciations in Patagonia. *Geol. Soc. Am. Bull.* **116**, 434-450 (2004).

Somoza, R. Updated Nazca (Farallon) – South America relative motions during the last 40 My: implications for mountain building in the central Andean region. *J. South Am. Earth Sci.* **11**, 211-215 (1998).

Stolar, D., Roe, G. & Willett, S. Controls on the patterns of topography and erosion rate in a critical orogen. *J. Geophys. Res.* **112**, F04002 (2007).

Thomson, S. N., Herve, F. & Stockhert, B. Mesozoic-Cenozoic denudation history of the Patagonian Andes (southern Chile) and its correlation to different subduction processes. *Tectonics* **20**, 693-711 (2001).

Thomson, S. N. Late Cenozoic geomorphic and tectonic evolution of the Patagonian Andes between latitudes 42 degrees S and 46 degrees S: An appraisal based on fission-track results from the transpressional intra-arc Liquine-Ofqui fault zone. *Geol. Soc. Am. Bull.* **114**, 1159-1173 (2002).

Thomson, S. N. & Herve, F. New time constraints for the age of metamorphism at the ancestral Pacific Gondwana margin of southern Chile (42-52 degrees S). *Rev. Geol. Chile* **29**, 255-271 (2002).

Tomkin, J. H. & Roe, G. H. Climate and tectonic controls on glaciated critical-taper orogens. *Earth Planet. Sci. Lett.* **262**, 385-397 (2007).

Whipple, K. X. & Meade, B. J. Orogen response to changes in climatic and tectonic forcing. *Earth Planet. Sci. Lett.* **243**, 218-228 (2006).

Willner, A. P., Herve, F., Thomson, S. N. & Massonne, H. J. Converging P-T paths of Mesozoic HP-LT metamorphic units (Diego de Almagro Island, Southern Chile): evidence for juxtaposition during late shortening of an active continental margin. *Mineral. Petrol.* **81**, 43-84 (2004).

Supplementary Table 1: New apatite fission-track data

Sample No.	Elevation (m)	Location		No. of Crystals	Track Density ($\times 10^6$ tr cm^{-2})			Age Dispersion	Central Age (Ma) ($\pm 1\sigma$)	Apatite Mean Track Length (μm $\pm$ 1 s.e.) (track no.)	Standard Deviation (μm)
		Latitude (°S)	Longitude (°W)		ρ_s (N_s)	ρ_i (N_i)	ρ_d (N_d)	($P\chi^2$)			
THC27	200	-45.6290	-72.4888	2	0.1509 (5)	1.690 (56)	1.064 (7343)	<0.01% (39%)	**16.8±7.9**	-	-
THC87	0	-49.5910	-75.4065	20	0.6168 (184)	4.717 (1407)	1.305 (9013)	0.5% (92%)	**30.6±2.7**	**13.44±0.29 (40)**	**1.81**
THC88	0	-49.5962	-75.3885	20	0.8712 (314)	6.334 (2283)	1.310 (9045)	<0.01% (99%)	**32.2±2.3**	**14.80±0.13 (91)**	**1.22**
THC89	100	-49.6050	-75.3790	20	0.1932 (167)	1.543 (1334)	1.315 (9077)	<0.01% (>99.9%)	**29.5±2.7**	**13.92±0.23 (24)**	**1.11**
THC90	0	-49.5932	-75.3710	20	1.892 (614)	13.22 (4290)	1.319 (9109)	<0.01% (95%)	**33.8±1.9**	**14.58±0.15 (100)**	**1.48**
THC92	0	-49.7077	-75.2495	8	0.1119 (17)	1.040 (158)	1.324 (9142)	<0.01% (96%)	**25.5±6.6**	-	-
THC93	0	-49.7135	-75.2120	20	0.7920 (490)	5.471 (3385)	1.329 (9174)	0.3% (83%)	**34.4±2.1**	**14.05±0.16 (100)**	**1.61**
THC94	0	-50.3378	-75.1963	20	1.269 (594)	5.957 (2789)	1.333 (9206)	<0.01% (83%)	**50.7±3.0**	**13.50±0.17 (100)**	**1.71**
THC95	0	-50.7883	-74.4238	20	0.6968 (306)	9.277 (4074)	1.338 (9238)	<0.01% (99%)	**18.0±1.3**	**14.95±0.11 (100)**	**1.12**
THC100	0	-49.5318	-73.8638	10	0.6458 (239)	12.95 (4793)	1.352 (9355)	<0.01% (82%)	**12.1±0.9**	**15.14±0.10 (100)**	**0.95**
THC101	0	-49.3005	-74.0448	20	0.0745 (32)	1.194 (513)	1.357 (9368)	<0.01% (99%)	**15.2±2.8**	**14.73±0.13 (56)**	**0.93**
THC102	0	-49.3568	-74.1075	20	0.0574 (56)	1.212 (1182)	1.361 (9400)	<0.01% (96%)	**11.6±1.6**	**15.13±0.17 (50)**	**1.16**
THC103	0	-49.5412	-74.1847	20	0.2819 (146)	5.322 (2756)	1.366 (2756)	<0.01% (99%)	**13.0±1.2**	**14.50±0.10 (100)**	**1.01**
THC104	0	-49.4243	-74.3005	20	0.4234 (307)	8.096 (5870)	1.370 (9464)	<0.01% (99%)	**12.8±0.9**	**14.99±0.11 (100)**	**1.06**
THC105	0	-48.6885	-74.5535	20	0.5925 (225)	9.711 (3688)	1.375 (9497)	<0.01% (99%)	**15.0±1.2**	**14.95±0.11 (100)**	**1.11**
THC106	0	-48.6167	-74.8240	20	0.2431 (139)	2.461 (1407)	1.380 (9529)	<0.01% (99%)	**24.4±2.4**	**15.00±0.14 (37)**	**0.85**
THC107	0	-48.5767	-74.9550	10	0.2676 (51)	2.839 (541)	1.384 (9561)	<0.01% (95%)	**23.4±3.5**	-	-
THC108	0	-48.5943	-75.0037	20	0.4513 (172)	5.016 (1912)	1.389 (9593)	<0.01% (99%)	**22.4±2.0**	**14.49±0.12 (91)**	**1.17**
THC109	0	-48.8025	-75.4655	20	1.737 (590)	7.836 (2662)	1.394 (9626)	0.1% (82%)	**55.2±3.2**	**13.52±0.23 (100)**	**2.27**
THC110	0	-48.8018	-75.4427	20	0.4557 (365)	2.413 (1933)	1.398 (9658)	<0.01% (85%)	**47.2±3.2**	**13.07±0.23 (100)**	**2.31**
THC111	0	-48.7695	-75.2022	20	0.4947 (235)	2.568 (1220)	1.403 (9690)	1.2% (70%)	**48.3±3.9**	**13.66±0.18 (100)**	**1.79**
THC112	0	-48.8340	-75.0518	20	0.2254 (80)	2.282 (810)	1.408 (9722)	0.1% (94%)	**24.9±3.1**	-	-
THC113	0	-48.7440	-74.9297	14	0.0843 (17)	1.037 (209)	1.325 (9149)	<0.01% (99%)	**19.3±4.9**	-	-
THC114	0	-48.7288	-73.9872	20	0.1004 (65)	1.877 (1216)	1.329 (9174)	<0.01% (99%)	**12.7±1.7**	**14.74±0.18 (47)**	**1.25**
THC115	0	-48.7278	-74.0458	20	0.3121 (125)	4.649 (1866)	1.332 (9199)	<0.01% (99%)	**16.0±1.6**	**14.41±0.17 (70)**	**1.37**
THC116	0	-48.7092	-74.3288	20	0.1288 (69)	1.891 (1013)	1.336 (9223)	<0.01% (99%)	**16.3±2.1**	**14.49±0.16 (46)**	**1.05**
THC117	0	-50.8458	-73.9458	20	0.2137 (157)	3.408 (2504)	1.339 (9248)	<0.01% (99%)	**15.0±1.4**	**15.06±0.11 (100)**	**1.07**
THC119	0	-50.7933	-73.8808	20	0.1532 (77)	3.046 (1531)	1.343 (9272)	<0.01% (96%)	**12.1±1.5**	**14.44±0.12 (56)**	**0.86**
THC120	0	-50.6687	-73.7705	17	0.0551 (28)	1.045 (531)	1.346 (9297)	<0.01% (98%)	**12.7±2.5**	-	-
THC121	0	-50.6825	-73.7952	15	0.0682 (45)	1.126 (743)	1.350 (9322)	<0.01% (99%)	**14.7±2.3**	-	-
THC122	0	-50.5088	-73.7158	20	0.1586 (150)	3.110 (2942)	1.354 (9346)	0.02% (98%)	**12.4±1.1**	**14.91±0.12 (100)**	**1.16**
THC123	0	-50.5892	-73.7520	20	0.0371 (23)	0.9725 (603)	1.357 (9371)	0.22% (92%)	**9.3±2.0**	-	-
THC124	0	-50.7817	-74.2575	20	0.2163 (92)	3.249 (1382)	1.361 (9396)	<0.01% (99%)	**16.2±1.9**	**14.27±0.11 (100)**	**1.12**
THC131	0	-51.7555	-74.1802	11	0.2874 (77)	3.703 (992)	1.368 (9445)	<0.01% (99%)	**19.0±2.4**	**14.73±0.14 (100)**	**1.37**
THC132	0	-52.0415	-73.7443	5	0.2317 (16)	3.345 (231)	1.371 (9469)	<0.01% (88%)	**17.0±4.4**	-	-
THC133	0	-52.0808	-73.7175	3	0.0579 (4)	0.5358 (37)	1.375 (9494)	0.02% (42%)	**26.6±14.0**	-	-
THC134	0	-52.2562	-73.5897	7	0.0947 (17)	2.339 (420)	1.378 (9519)	0.24% (61%)	**10.0±2.5**	-	-

Supplementary Table 1: New apatite fission-track data

Sample No.	Elevation (m)	Location		No. of Crystals	Track Density ($\times 10^6$ tr cm^{-2})			Age Dispersion	Central Age (Ma) (±1σ)	Apatite Mean Track Length	Standard Deviation
		Latitude (°S)	Longitude (°W)		ρ_s (N_s)	ρ_i (N_i)	ρ_d (N_d)	($P\chi^2$)		(μm ± 1 s.e.) (track no.)	(μm)
THC135	10	-42.9133	-72.7125	20	0.0590 (34)	2.514 (1448)	1.369 (9456)	0.64% (86%)	**5.8±1.0**	**14.19±0.27 (21)**	**1.19**
THC136	1060	-46.0823	-72.0510	3	0.1334 (7)	5.317 (279)	1.373 (9480)	<0.01% (47%)	**6.2±2.4**		**-**
THC137	1211	-46.0657	-72.0413	8	0.3103 (42)	0.8867 (120)	1.376 (9504)	<0.01% (78%)	**85.8±15.7**	**14.50±0.27 (8)**	**0.72**
THC138	912	-46.1003	-72.0495	20	0.4916 (406)	1.332 (1092)	1.380 (9528)	6.05% (23%)	**91.3±6.4**	**14.39±0.10 (100)**	**0.99**
THC139	506	-46.1102	-72.1180	15	0.3264 (128)	9.306 (365)	1.383 (9552)	<0.01% (99%)	**86.4±9.4**	**13.86±0.20 (30)**	**1.09**
THC140	325	-46.1255	-72.1667	20	0.1943 (117)	0.5929 (357)	1.387 (9576)	<0.01% (99%)	**81.0±9.1**	**14.92±0.31 (19)**	**1.33**
THC141	811	-45.9887	-71.9090	15	0.3456 (158)	0.8969 (410)	1.390 (9600)	<0.01% (98%)	**95.4±9.6**	**14.76±0.15 (54)**	**1.07**
THC142	89	-45.3535	-72.4572	20	0.0512 (27)	1.234 (651)	1.394 (9624)	<0.01% (95%)	**10.4±2.1**	**-**	**-**
THC143	100	-45.2930	-72.3263	20	0.2632 (149)	1.443 (817)	1.355 (9353)	<0.01% (99%)	**44.2±4.3**	**12.25±0.29 (42)**	**1.85**
THC144	362	-45.2330	-72.2313	16	0.2460 (107)	0.7517 (327)	1.346 (9291)	0.03% (92%)	**78.5±9.2**	**11.68±0.20 (100)**	**2.02**
THC145	275	-44.9317	-72.1630	20	0.0429 (20)	1.114 (520)	1.337 (9229)	0.01% (92%)	**9.2±2.1**	**-**	**-**
THC146	43	-44.4618	-72.5773	20	0.0223 (19)	1.488 (1266)	1.328 (9167)	0.15% (73%)	**3.6±0.8**	**-**	**-**
THC147	16	-44.4407	-72.5940	20	0.0262 (16)	1.899 (1159)	1.319 (9105)	6.8% (90%)	**3.3±0.8**	**-**	**-**
THC148	110	-44.4482	-72.5195	20	0.0792 (47)	5.128 (3045)	1.310 (9043)	0.23% (82%)	**3.6±0.6**	**14.90±0.18 (42)**	**1.18**
THC150	110	-44.4482	-72.5195	20	0.0278 (17)	2.315 (1416)	1.301 (8981)	34% (18%)	**2.8±0.7**	**-**	**-**
THC151	0	-52.1085	-73.9033	20	0.2209 (126)	3.345 (1908)	1.292 (8919)	<0.01% (95%)	**15.3±1.5**	**15.07±0.11 (100)**	**1.11**
THC152	0	-52.1452	-74.0403	20	0.1481 (81)	2.273 (1243)	1.283 (8857)	<0.01% (97%)	**15.0±1.8**	**15.11±0.11 (100)**	**1.09**
THC153	0	-52.1008	-74.2353	20	0.1275 (56)	1.671 (734)	1.274 (8795)	0.01% (97%)	**17.4±2.5**	**14.03±0.18 (72)**	**1.51**
THC154	0	-51.7958	-74.7703	20	0.8167 (441)	3.891 (2101)	1.265 (8733)	0.04% (91%)	**47.5±3.0**	**14.08±0.19 (100)**	**1.90**
THC155	0	-51.7860	-74.9705	15	1.009 (312)	5.072 (1569)	1.256 (8671)	11.6% (46%)	**45.6±3.7**	**13.24±0.17 (100)**	**1.70**
THC156	50	-51.8632	-74.7913	20	0.2126 (128)	1.126 (678)	1.247 (8609)	0.04% (96%)	**42.1±4.4**	**13.52±0.17 (100)**	**1.70**
THC157	10	-51.9517	-74.8327	20	0.3799 (181)	1.308 (623)	1.238 (8547)	<0.01% (99%)	**64.2±5.9**	**12.95±0.20 (100)**	**2.03**
THC158	10	-52.0087	-74.9220	20	0.6845 (380)	2.217 (1231)	1.229 (8485)	0.16% (72%)	**67.7±4.7**	**13.49±0.14 (100)**	**1.44**
THC159	10	-51.9720	-74.8062	20	0.4568 (270)	1.712 (1012)	1.220 (8423)	0.01% (91%)	**58.1±4.5**	**13.34±0.18 (100)**	**1.79**
Pancho4	0	-44.0403	-73.6297	20	0.1363 (83)	0.7077 (431)	1.141 (7880)	<0.01% (99%)	**39.3±4.9**	**-**	**-**
Pancho6	0	-44.0350	-73.6050	12	0.1117 (27)	0.5710 (138)	1.139 (7863)	2.23% (62%)	**39.9±8.5**	**-**	**-**
TP0127	0	-46.8000	-75.6000	20	0.0152 (11)	1.718 (1243)	1.164 (8040)	3.2% (61%)	**1.9±0.6**	**-**	**-**
TP0128B	0	-46.8167	-75.6167	20	0.0239 (15)	1.735 (1090)	1.166 (8052)	0.02% (97.3)	**2.9±0.8**	**-**	**-**
TP0137	0	-46.7667	-75.5167	10	0.0222 (6)	1.478 (400)	1.168 (8064)	1.5% (60%)	**3.1±1.3**	**-**	**-**
SP06b	400	-41.4933	-72.4150	20	0.6194 (136)	21.87 (4803)	1.170 (8075)	<0.01% (99%)	**5.9±0.6**	**14.42±0.12 (100)**	**1.19**
SP011	25	-41.7300	-72.6000	20	0.0829 (26)	3.423 (1073)	1.171 (8087)	<0.01% (98%)	**5.1±1.0**	**14.64±0.14 (100)**	**1.36**
SP040	1675	-41.8000	-71.8983	18	0.1362 (38)	2.201 (614)	1.173 (8099)	<0.01% (99%)	**13.0±2.2**	**15.50±0.40 (7)**	**0.98**
SP041	1525	-41.8617	-71.8883	13	0.1541 (20)	2.288 (297)	1.175 (8111)	0.03% (87%)	**14.2±3.3**	**14.71±0.24 (26)**	**1.22**
SP043	1520	-42.0267	-71.7600	20	0.5874 (202)	1.669 (574)	1.176 (8123)	0.97% (61%)	**73.8±6.6**	**13.36±0.16 (100)**	**1.63**
SP046	1450	-42.0617	-72.1300	20	0.0761 (43)	4.801 (2712)	1.178 (8135)	<0.01% (98%)	**3.4±0.5**	**14.74±0.19 (76)**	**1.66**
SP048	275	-41.9033	-71.9283	16	0.1886 (31)	2.836 (466)	1.180 (8147)	<0.01% (99%)	**14.1±2.7**	**15.08±0.28 (11)**	**0.88**

Supplementary Table 1: New apatite fission-track data

Sample No.	Elevation (m)	Location		No. of Crystals	Track Density ($\times 10^6$ tr cm^{-2})			Age Dispersion	Central Age (Ma) (±1σ)	Apatite Mean Track Length (μm ± 1 s.e.) (track no.)	Standard Deviation (μm)
		Latitude (°S)	Longitude (°W)		ρ_s (N_s)	ρ_i (N_i)	ρ_d (N_d)	($P\chi^2$)			
SP057	1325	-41.3950	-72.0300	10	0.0920 (10)	6.081 (613)	1.182 (8158)	<0.01% (95%)	**3.5±1.1**	**15.13±0.23 (6)**	**0.51**
SP061	1650	-41.9950	-72.3367	20	0.1177 (33)	6.456 (1810)	1.183 (8170)	<0.01% (99%)	**3.9±0.7**	**14.62±0.27 (21)**	**1.20**
SP062	1325	-42.0717	-72.3300	20	0.1943 (110)	8.394 (4753)	1.185 (8182)	23.97% (7%)	**5.1±0.6**	**15.07±0.13 (55)**	**0.95**
SP066	125	-41.9467	-72.3733	20	0.0229 (7)	2.389 (729)	1.187 (8194)	1.13% (62%)	**2.0±0.8**	**14.36±0.59 (9)**	**1.66**
SP067	250	-41.4083	-72.6467	20	0.1329 (49)	2.780 (1025)	1.188 (8206)	0.03% 90%	**10.2±1.5**	**15.01±0.12 (84)**	**1.05**
SP069	650	-43.5483	-72.9667	8	0.1502 (28)	3.781 (705)	1.190 (8218)	<0.01% (99%)	**8.5±1.7**	**-**	**-**
SP070	1450	-43.5167	-72.7717	20	0.1134 (52)	3.734 (1712)	1.192 (8230)	<0.01% (99%)	**6.5±1.0**	**15.39±0.11 (100)**	**1.11**
SP071	1350	-43.5533	-72.6950	20	0.1027 (61)	6.446 (3828)	1.194 (8241)	0.19% (82%)	**3.4±0.5**	**14.87±0.27 (27)**	**1.36**
SP072	1490	-43.6117	-72.5117	20	0.0688 (27)	3.855 (1512)	1.195 (8253)	0.70% (76%)	**3.8±0.8**	**14.97±0.16 (35)**	**0.94**
SP074	1625	-43.6533	-72.2550	20	0.5805 (194)	2.498 (835)	1.197 (8265)	16.30% (26%)	**49.5±4.8**	**12.02±0.25 (100)**	**2.52**
SP075	1670	-43.7033	-72.0483	10	0.5871 (60)	2.936 (300)	1.199 (8277)	20.08% (56%)	**41.5±6.9**	**12.94±0.94 (9)**	**2.66**
SP076	1500	-43.7083	-71.9167	20	1.122 (364)	4.061 (1318)	1.200 (8289)	<0.01% (99%)	**59.2±4.1**	**13.08±0.12 (100)**	**1.21**
SP080	1275	-43.0817	-72.5550	20	0.1703 (91)	11.50 (6145)	1.202 (8301)	0.25% (73%)	**3.2±0.4**	**14.79±0.30 (37)**	**1.83**
SP081	1725	-43.2183	-72.1033	20	0.1648 (61)	5.298 (1961)	1.204 (8313)	3.54% (72%)	**6.7±0.9**	**14.81±0.15 (100)**	**1.47**
SP082	1700	-43.3033	-71.8850	20	0.3702 (68)	3.011 (553)	1.206 (8324)	40.87% (3%)	**28.6±5.0**	**14.50±0.31 (19)**	**1.32**
SP083	1650	-43.4500	-72.1717	20	0.2504 (178)	5.328 (3745)	1.207 (8336)	0.86% (74%)	**10.2±0.9**	**14.08±0.18 (100)**	**1.82**
SP084	100	-43.4350	-72.1367	20	0.0646 (39)	3.594 (2169)	1.209 (8348)	0.01% (96%)	**3.9±0.7**	**15.38±0.24 (9)**	**0.69**
SP095	25	-43.9017	-72.8133	20	0.0901 (24)	3.696 (985)	1.267 (8747)	<0.01% (96%)	**5.5±1.2**	**14.97±0.44 (20)**	**1.91**
SP096	25	-44.0033	-72.6667	20	0.0778 (51)	8.781 (5760)	1.263 (8724)	0.02% (88%)	**2.0±0.3**	**15.19±0.23 (31)**	**1.27**
SP111	75	-43.7033	-72.2800	11	0.0773 (11)	5.322 (757)	1.260 (8700)	0.30% (70%)	**3.3±1.0**	**-**	**-**
SP112	75	-43.7183	-72.2750	20	0.0370 (18)	1.374 (668)	1.256 (8676)	0.34% (89%)	**6.1±1.5**	**15.07±0.29 (19)**	**1.21**
SP113	75	-43.7367	-72.2850	20	0.0611 (20)	2.285 (748)	1.253 (8652)	0.01% (95%)	**6.0±1.4**	**14.72±0.26 (26)**	**1.31**
SP115	0	-45.0433	-73.7317	20	0.5526 (174)	2.950 (929)	1.250 (8629)	<0.01% (99%)	**41.9±3.8**	**13.60±0.18 (100)**	**1.76**
SP124	0	-44.7833	-73.3450	20	0.1712 (35)	1.869 (382)	1.246 (8605)	<0.01% (99%)	**20.5±3.7**	**14.98±0.30 (17)**	**1.18**
SP125	0	-45.0600	-73.4083	20	0.3351 (118)	3.831 (1349)	1.243 (8581)	<0.01% (99%)	**19.5±2.0**	**14.93±0.10 (100)**	**1.02**
SP128	300	-42.0300	-71.5683	20	0.3918 (145)	4.139 (1532)	1.239 (8567)	1.26% (62%)	**21.0±2.0**	**14.02±0.17 (100)**	**1.72**
SP133	250	-41.0979	-71.4300	20	0.2463 (83)	3.888 (1310)	1.236 (8533)	<0.01% (99%)	**14.0±1.7**	**14.23±0.16 (100)**	**1.64**
SP137	450	-41.5783	-71.7767	20	0.0359 (11)	0.6320 (195)	1.232 (8510)	<0.01% (95%)	**12.5±3.9**	**14.10±0.76 (3)**	**1.08**
SP139	300	-41.5933	-71.6117	20	0.5746 (123)	3.153 (675)	1.229 (8486)	49.45% (0.5%)	**28.1±5.2**	**13.07±0.39 (56)**	**2.88**
GCH02	225	-42.6683	-72.5800	20	0.1060 (30)	4.239 (1200)	1.225 (8462)	<0.01% (89%)	**5.5±1.0**	**15.13±0.32 (10)**	**0.96**
AZ16	430	-43.2500	-71.9333	20	0.0447 (10)	3.120 (698)	1.222 (8438)	<0.01% (99%)	**3.1±1.0**	**15.14±0.29 (18)**	**1.21**
LLA1	984	-38.7166	-71.6208	20	0.1368 (66)	3.503 (1690)	1.873 (5844)	<0.01% (99%)	**12.9±1.7**	**-**	**-**
LLA4	1870	-38.7366	-71.5537	20	0.1392 (100)	4.050 (2909)	1.856 (5793)	<0.01% (99%)	**11.2±1.2**	**-**	**-**
LLA6	1709	-38.7302	-71.5397	12	0.0577 (12)	2.011 (418)	1.840 (5741)	0.01% (76%)	**9.3±2.7**	**-**	**-**
LOF19	1050	-39.8305	-71.8314	20	0.1011 (84)	3.692 (3067)	1.823 (5690)	<0.01% (99%)	**8.8±1.0**	**-**	**-**
LOF64	670	-39.7342	-71.8231	20	0.0093 (5)	1.078 (582)	1.807 (5639)	5.47% (86%)	**2.7±1.2**	**-**	**-**

Supplementary Table 1: New apatite fission-track data

Sample No.	Elevation (m)	Location		No. of Crystals	Track Density (x 10^6 tr cm^{-2})			Age Dispersion	Central Age (Ma) (±1σ)	Apatite Mean Track Length	Standard Deviation
		Latitude (°S)	Longitude (°W)		ρ_s (N_s)	ρ_i (N_i)	ρ_d (N_d)	($P\chi^2$)		(μm ± 1 s.e.) (track no.)	(μm)
LOF67	750	-39.7344	-71.6945	20	0.0398 (37)	2.377 (2212)	1.790 (5587)	<0.01% (99%)	**5.3±0.9**	-	-
LOF95	880	-39.6466	-71.8134	20	0.1096 (56)	8.102 (4141)	1.774 (5536)	0.01% (94%)	**4.2±0.6**	-	-
LOF150	1300	-38.6676	-71.3874	20	0.4138 (188)	3.590 (1631)	1.758 (5484)	<0.01% (99%)	**35.6±3.0**	**11.89±0.22 (100)**	**2.23**
LOF151	1450	-38.7067	-71.4700	20	0.0922 (74)	1.950 (1565)	1.741 (5433)	<0.01% (95%)	**14.5±1.8**	**13.00±0.53 (20)**	**2.32**
LOF155	1180	-38.8021	-71.2714	20	0.6686 (300)	3.118 (1399)	1.725 (5382)	<0.01% (99%)	**64.9±4.8**	**13.66±0.12 (100)**	**1.23**
LOF158	550	-38.8524	-71.5969	20	0.0054 (3)	0.8264 (459)	1.708 (5330)	0.04% (99%)	**2.0±1.1**	-	-
LOF167	2270	-38.5994	-70.8287	20	0.2029 (88)	0.8991 (390)	1.692 (5279)	<0.01% (98%)	**66.9±8.3**	-	-
LOF169	950	-38.4542	-71.3030	20	0.1464 (53)	3.807 (1378)	1.675 (5227)	<0.01% (99%)	**11.3±1.6**	-	-
06PA02	1490	-38.6559	-71.6014	20	0.0895 (46)	1.771 (911)	1.445 (4508)	1.9fi (65%)	**12.8±2.0**	-	-
06PA03	1334	-38.6542	-71.6021	20	0.2571 (138)	5.791 (3108)	1.428 (4456)	<0.01% (92%)	**11.2±1.1**	-	-
FO02-07	1	-53.1567	-73.2935	11	0.1509 (37)	2.262 (644)	1.798 (5610)	<0.01% (99%)	**18.2±3.1**	-	-
FO02-11	1	-52.9752	-72.9528	15	0.2015 (64)	3.220 (1023)	1.788 (5579)	<0.01% (>99.9%)	**19.7±2.6**	-	-
FO02-18	1	-52.7265	-73.3678	20	0.0652 (59)	1.042 (943)	1.778 (5548)	<0.01% (>99.9%)	**19.6±2.7**	-	-
FO03-26	1	-52.4175	-73.7598	20	0.0803 (48)	1.350 (807)	1.768 (5517)	<0.01% (>99.9%)	**18.5±2.8**	-	-
FO03-28	1	-52.4110	-73.7437	20	0.1328 (62)	2.226 (1039)	1.758 (5486)	<0.01% (>99.9%)	**18.5±2.5**	-	-
FO03-31	1	-53.3450	-73.1035	20	0.0658 (40)	1.104 (671)	1.748 (5455)	<0.01% (99%)	**18.3±3.1**	-	-
FO03-32	1	-53.4297	-72.9127	20	0.0682 (46)	1.051 (709)	1.738 (5424)	<0.01% (99%)	**19.8±3.1**	-	-
FO03-33	1	-53.5700	-72.4032	20	0.0625 (32)	1.000 (512)	1.728 (5393)	<0.01% (99%)	**19.0±3.5**	-	-
FO03-50	1	-53.5327	-72.3527	20	0.0525 (35)	0.8552 (570)	1.718 (5362)	<0.01% (99%)	**18.6±3.3**	-	-
FO04-08	1	-50.4710	-74.1135	20	0.2651 (111)	4.255 (1782)	1.708 (5331)	<0.01% (99%)	**18.7±2.0**	-	-
FO04-15	1	-50.5352	-73.8967	20	0.0553 (4)	0.8978 (65)	1.698 (5300)	<0.01% (91%)	**18.4±9.5**	-	-
FO04-18	1	-50.4152	-74.5520	20	0.3158 (178)	4.979 (2806)	1.689 (5269)	<0.01% (>99.9%)	**18.9±1.6**	**14.74±0.10 (72)**	**0.84**
FO06-05	800	-39.7644	-71.7810	20	0.0719 (34)	2.253 (1066)	1.639 (5114)	<0.01% (99%)	**9.2±1.6**	-	-
FO06-09	378	-39.7564	-71.8312	14	0.0796 (15)	4.016 (757)	1.629 (5083)	0.04% (85%)	**5.7±1.5**	-	-
FO06-13	18	-39.8110	-72.9425	7	0.5076 (51)	1.752 (176)	1.619 (5052	<0.01% (86%)	**82.1±13.4**	-	-
FO06-14	1	-55.9759	-67.2893	20	0.2978 (134)	0.8378 (377)	1.609 (5021)	<0.01% (99%)	**100.0±10.7**	-	-
07BA25	10	-51.4157	-73.1095	20	0.0343 (33)	0.4905 (472)	1.530 (472)	0.08% (89%)	**18.8±3.5**	-	-

Notes:
(i). Analyses by external detector method using 0.5 for the 4π/2π geometry correction factor;
(ii). Ages calculated using dosimeter glass: IRMM540R with ζ_{540R} = 352.4±12.1
(except sample THC27 where dosimeter glass CN5 was used with ζ_{CN5} = 354.1±5.6);
(iii). $P\chi^2$ is the probability of obtaining a χ^2 value for v degrees of freedom where v = no. of crystals - 1;
(iv) Latitude and Longitude based on WGS84 geoid.

Supplementary Table 2: New apatite (U-Th)/He data

Sample	Latitude	Longitude	Elevation (m)	Corrected Age (Ma)	±2σ (Ma)	Ft	No of Grains	mass (μg)	mwar (μm)	U (ppm)	Th (ppm)	Th/U	He (ncc)
LLA1	-38.7166	-71.6208	984	**3.03**	**0.18**	0.706	1	2.14	44.5	40.8	76.9	1.93	0.0327
LLA4	-38.7366	-71.5537	1870	**7.30**	**0.44**	0.619	1	1.33	31.5	34.5	24.2	0.719	0.0005
LLA6	-38.7302	-71.5397	1709	**6.84**	**0.41**	0.667	2	3.54	41.1	12.1	47.7	4.05	0.0466
LOF19	-39.8305	-71.8314	1050	**2.18**	**0.13**	0.670	1	1.54	39.8	12.0	39.1	3.33	0.0059
LOF67	-39.7344	-71.6945	750	**2.39**	**0.14**	0.765	1	5.48	58.5	11.8	28.1	2.45	0.0228
LOF95	-39.6466	-71.8134	880	**2.26**	**0.14**	0.714	2	5.22	47.7	23.6	43.8	1.90	0.0346
LOF135	-39.0444	-71.8023	370	**0.98**	**0.06**	0.679	1	1.62	40.5	23.7	4.48	0.194	0.0032
LOF149	-38.5960	-71.4385	1350	**3.45**	**0.21**	0.729	1	3.63	48.8	13.9	25.0	1.84	0.0222
LOF150	-38.6676	-71.3874	1300	**4.30**	**0.26**	0.738	1	4.34	50.5	32.1	81.2	2.59	0.0859
LOF151	-38.7067	-71.4700	1450	**4.39**	**0.26**	0.797	1	9.56	67.5	15.0	44.5	3.05	0.1042
LOF155	-38.8021	-71.2714	1180	**12.50**	**0.75**	0.772	2	9.09	56.2	27.0	29.3	1.12	0.3630
LOF158	-38.8524	-71.5969	550	**1.42**	**0.09**	0.704	1	3.51	43.8	4.73	18.1	3.93	0.0040
LOF163	-38.6182	-71.0155	1180	**10.99**	**0.66**	0.698	1	3.03	45.3	2.95	26.4	9.17	0.0265
LOF167	-38.5994	-70.8287	2270	**48.61**	**2.92**	0.752	1	3.73	54.3	4.78	12.4	2.66	0.1338
LOF167r1	-38.5994	-70.8287	2270	**60.16**	**3.61**	0.668	1	1.64	42.5	4.25	18.3	4.42	0.0738
LOF169	-38.4542	-71.3030	950	**7.43**	**0.45**	0.742	1	3.15	53.8	41.7	27.1	0.667	0.1015
LOF171	-38.5535	-71.2795	1270	**1.84**	**0.11**	0.734	1	3.26	59.5	0.970	10.6	11.2	0.0019
VAL10	-39.6885	-73.3471	370	**23.87**	**1.43**	0.652	2	2.55	34.5	14.4	23.4	1.67	0.0978
VAL14	-39.9029	-73.4979	30	**32.59**	**1.96**	0.561	2	1.78	28.5	18.0	22.2	1.27	0.0943
VAL20	-39.4191	-72.7203	90	**8.82**	**0.53**	0.759	1	3.80	60.3	37.3	42.7	1.17	0.0016
SP70	-43.5167	-72.7717	1450	**2.20**	**0.07**	0.732	1	3.63	47.8	20.9	49.8	2.45	0.0231
SP70r1	-43.5167	-72.7717	1450	**3.52**	**0.26**	0.685	1	1.81	43.8	66.3	124	1.92	0.0506
SP71	-43.5533	-72.6950	1350	**1.80**	**0.06**	0.665	1	1.45	37.8	64.5	0.342	0.00545	0.0136
SP71r1	-43.5533	-72.6950	1350	**3.95**	**0.73**	0.692	1	2.30	45.5	17.5	0.251	0.0147	0.0135
SP72	-43.6117	-72.5117	1490	**1.84**	**0.06**	0.699	1	2.75	40.3	43.3	39.5	0.936	0.0226
SP72r1	-43.6117	-72.5117	1490	**2.41**	**0.34**	0.681	1	2.10	40.3	33.3	46.2	1.42	0.0185
SP74	-43.6533	-72.2550	1625	**2.45**	**0.08**	0.646	1	1.25	35.0	41.9	53.8	1.32	0.0131
SP74r1	-43.6533	-72.2550	1625	**5.49**	**0.77**	0.635	1	1.55	34.3	22.1	42.1	1.95	0.0211
SP75	-43.7033	-72.0483	1670	**4.55**	**0.17**	0.669	1	1.69	41.8	8.99	34.1	3.89	0.0108
SP75r1	-43.7033	-72.0483	1670	**4.02**	**1.34**	0.595	1	0.80	32.8	25.5	58.4	2.35	0.0092
SP76	-43.7083	-71.9167	1500	**23.30**	**0.71**	0.640	1	1.82	39.3	5.52	24.2	4.50	0.0384
SP76r1	-43.7083	-71.9167	1500	**14.70**	**2.12**	0.550	1	0.70	27.5	15.9	41.3	2.67	0.0179
SP80	-43.0817	-72.5550	1275	**1.63**	**0.05**	0.736	1	3.32	49.3	100	26.1	0.267	0.0514
SP80r1	-43.0817	-72.5550	1275	**1.55**	**0.22**	0.742	1	3.44	51.8	46.9	23.3	0.511	0.0251
SP81	-43.2183	-72.1033	1725	**2.52**	**0.07**	0.762	1	5.51	53.8	40.3	78.5	2.00	0.0754
SP81r1	-43.2183	-72.1033	1725	**3.04**	**0.09**	0.673	1	1.99	40.0	34.8	81.0	2.39	0.0266
SP83	-43.3033	-71.8850	1700	**3.62**	**0.10**	0.751	1	3.78	53.0	46.7	95.9	2.11	0.0864
SP83r1	-43.3033	-71.8850	1700	**3.79**	**0.11**	0.655	1	2.00	39.5	49.0	98.4	2.06	0.0435
SP84	-43.4500	-72.1717	1650	**1.82**	**0.06**	0.655	1	1.64	36.5	32.3	100.0	3.17	0.0133
SP84r1	-43.4500	-72.1717	1650	**2.38**	**0.12**	0.695	1	2.12	45.5	9.57	26.1	2.79	0.0067
SP95	-43.9017	-72.8133	25	**1.28**	**0.07**	0.617	1	1.14	31.8	26.8	50.1	1.91	0.0042
SP95r1	-43.9017	-72.8133	25	**0.79**	**0.65**	0.655	1	1.53	37.3	34.2	46.1	1.38	0.0043
SP96	-44.0033	-72.6667	25	**1.15**	**0.04**	0.690	1	2.43	40.8	62.4	66.9	1.10	0.0182
SP96r1	-44.0033	-72.6667	25	**1.39**	**0.05**	0.668	1	1.87	43.0	83.6	63.5	0.779	0.0207
SP111	-43.7033	-72.2800	75	**1.46**	**0.04**	0.681	1	1.98	41.8	51.6	112	2.23	0.0187
SP111r1	-43.7033	-72.2800	75	**1.53**	**0.54**	0.601	1	1.32	32.0	24.7	33.1	1.37	0.0048
SP112	-43.7183	-72.2750	75	**2.94**	**0.09**	0.778	1	7.35	68.3	10.8	17.3	1.63	0.0309
SP112r1	-43.7183	-72.2750	75	**2.03**	**0.07**	0.723	1	2.33	50.0	16.2	50.6	3.20	0.0118
SP113	-43.7367	-72.2850	75	**2.56**	**0.11**	0.673	1	1.98	49.0	9.48	19.8	2.14	0.0060
SP113r1	-43.7367	-72.2850	75	**1.37**	**0.12**	0.629	1	1.23	34.8	16.6	31.6	1.95	0.0031
06PA02	-38.6559	-71.6014	1490	**4.32**	**0.12**	0.746	1	4.20	50.0	20.3	30.0	1.52	0.0458
06PA02r1	-38.6559	-71.6014	1490	**4.60**	**0.27**	0.763	1	6.09	61.5	18.4	22.8	1.27	0.0629
06PA03	-38.6542	-71.6021	1334	**5.88**	**0.18**	0.678	1	1.38	42.8	96.2	19.6	0.209	0.0673
06PA03r1	-38.6542	-71.6021	1334	**5.05**	**0.17**	0.607	1	0.80	32.3	88.8	17.3	0.200	0.0276
06PA04	-46.5476	-72.9149	260	**4.25**	**0.12**	0.692	1	2.41	41.3	33.9	100	3.04	0.0497
06PA04r1	-46.5476	-72.9149	260	**4.89**	**0.13**	0.796	1	10.92	71.0	49.6	101	2.10	0.3812
06PA05	-46.5007	-73.1497	151	**4.69**	**0.18**	0.617	1	1.36	33.5	8.06	36.8	4.69	0.0084
06PA06	-46.4886	-73.0934	146	**5.63**	**0.31**	0.599	1	1.06	32.0	7.44	27.6	3.81	0.0063

Supplementary Table 2: New apatite (U-Th)/He data

Sample	Latitude	Longitude	Elevation (m)	Corrected Age (Ma)	±2σ (Ma)	Ft	No of Grains	mass (μg)	mwar (μm)	U (ppm)	Th (ppm)	Th/U	He (ncc)
06PA08	-46.5172	-73.0101	166	**4.26**	**0.13**	0.672	1	1.67	40.0	61.7	69.2	1.15	0.0453
06PA08r1	-46.5172	-73.0101	166	**3.98**	**0.12**	0.664	1	1.97	40.5	86.5	68.6	0.813	0.0647
06PA09	-46.5330	-72.9575	216	**3.93**	**0.12**	0.669	1	1.95	37.3	49.9	96.7	1.99	0.0453
06PA09r1	-46.5330	-72.9575	216	**3.51**	**0.10**	0.643	1	2.02	36.5	51.1	92.4	1.86	0.0403
06PA10	-48.1038	-72.9268	127	**8.74**	**0.27**	0.663	1	1.74	43.3	45.6	32.7	0.736	0.0657
06PA11	-48.1072	-72.9308	118	**7.64**	**0.30**	0.542	1	0.66	28.8	32.3	26.8	0.850	0.0128
06PA11r1	-48.1072	-72.9308	118	**6.16**	**0.16**	0.690	1	2.65	46.5	47.5	97.0	2.10	0.0965
06PA13	-48.1894	-72.7571	299	**4.79**	**0.15**	0.747	1	3.55	53.3	19.7	8.17	0.425	0.0339
06PA13r1	-48.1894	-72.7571	299	**5.24**	**0.17**	0.766	1	3.97	55.3	29.8	9.38	0.323	0.0619
06PA14	-48.2585	-72.6896	263	**4.76**	**0.51**	0.691	1	2.18	42.5	1.19	5.61	4.83	0.0022
06PA14r1	-48.2585	-72.6896	263	**5.99**	**0.40**	0.741	1	3.86	54.0	0.514	6.63	13.2	0.0044
06PA15	-48.2767	-72.6818	270	**4.83**	**0.30**	0.623	1	1.20	35.0	5.97	22.0	3.78	0.0049
06PA16	-47.7947	-73.5289	50	**7.07**	**0.25**	0.617	1	0.99	31.0	38.5	17.4	0.463	0.0225
06PA17	-47.7716	-73.3460	42	**6.04**	**0.21**	0.578	1	1.02	29.8	14.3	67.4	4.83	0.0134
06PA18	-48.1165	-72.8837	412	**7.08**	**0.21**	0.678	1	2.28	44.8	12.0	21.7	1.86	0.0236
06PA19	-48.1507	-72.7989	308	**8.79**	**0.29**	0.697	1	2.50	50.0	11.3	12.3	1.11	0.0265
06PA19r1	-48.1507	-72.7989	308	**5.57**	**0.18**	0.719	1	3.09	51.0	34.9	5.19	0.153	0.0543
06PA52	-43.3102	-71.9520	613	**2.43**	**0.09**	0.671	1	2.84	43.3	4.17	39.3	9.65	0.0076
06PA52r1	-43.3102	-71.9520	613	**2.97**	**0.09**	0.649	1	1.33	38.0	25.5	172	6.90	0.0205
06PA54	-43.3183	-71.9414	701	**4.02**	**0.39**	0.544	1	0.80	29.3	5.78	19.5	3.46	0.0022
06PA54r1	-43.3183	-71.9414	701	**3.09**	**0.72**	0.707	1	2.34	45.8	3.86	16.4	4.34	0.0049
06PA55	-43.2523	-71.9405	421	**3.73**	**0.52**	0.661	1	2.00	40.0	0.817	7.28	9.13	0.0017
06PA55r1	-43.2523	-71.9405	421	**3.86**	**0.24**	0.731	1	3.25	48.5	30.2	17.8	0.606	0.0386
06PA56	-43.3492	-72.0365	190	**5.18**	**0.12**	0.711	1	3.46	43.5	25.6	33.7	1.35	0.0522
06PA56r1	-43.3492	-72.0365	190	**2.43**	**0.12**	0.657	1	1.77	37.5	12.2	29.8	2.51	0.0067
06PA57	-43.4735	-72.1091	147	**4.51**	**0.10**	0.750	1	4.28	57.0	15.3	63.7	4.27	0.0542
06PA57r1	-43.4735	-72.1091	147	**2.37**	**0.06**	0.776	1	7.28	61.3	19.3	75.0	3.99	0.0609
06PA60	-51.8598	-73.8093	1	**13.58**	**0.31**	0.710	1	2.67	48.0	18.3	65.5	3.67	0.1063
06PA60r1	-51.8598	-73.8093	1	**9.49**	**0.36**	0.633	1	1.00	35.5	7.95	21.8	2.81	0.0098
06PA61	-50.2429	-74.6715	1	**13.77**	**0.32**	0.686	1	2.46	41.0	22.0	48.2	2.25	0.0955
06PA61r1	-50.2429	-74.6715	1	**14.24**	**0.37**	0.649	1	1.76	39.8	44.5	76.9	1.77	0.1241
06PA62	-49.6479	-73.7405	1	**23.07**	**0.58**	0.608	1	1.27	34.5	13.4	24.8	1.91	0.0424
06PA62r1	-49.6479	-73.7405	1	**16.09**	**0.45**	0.708	1	1.87	47.0	8.18	18.7	2.35	0.0331
06PA63	-49.6116	-73.8333	1	**25.53**	**0.69**	0.574	1	1.18	35.0	0.240	110	470	0.0554
06PA63r1	-49.6116	-73.8333	1	**16.58**	**1.63**	0.603	1	1.11	39.0	13.3	51.6	3.99	0.0343
06PA64	-49.5511	-73.8929	1	**27.68**	**0.73**	0.612	1	1.63	39.3	0.174	86.8	512	0.0694
06PA65	-49.5632	-73.9821	1	**11.18**	**0.28**	0.755	1	4.13	53.0	61.0	4.38	0.0736	0.2622
06PA65r1	-49.5632	-73.9821	1	**4.04**	**0.13**	0.679	1	1.56	40.8	72.5	7.17	0.102	0.0383
06PA66	-49.3764	-74.0633	1	**15.27**	**0.37**	0.657	1	1.27	39.0	27.7	23.2	0.856	0.0524
06PA66r1	-49.3764	-74.0633	1	**14.44**	**0.88**	0.691	1	1.97	42.3	21.1	14.3	0.694	0.0596
06PA67	-49.5638	-74.1366	1	**28.42**	**0.71**	0.636	1	1.15	35.3	26.4	20.6	0.801	0.0791
06PA67r1	-49.5638	-74.1366	1	**22.00**	**0.67**	0.629	1	1.38	37.0	13.3	13.3	1.03	0.0386
06PA68	-49.5987	-74.2301	1	**14.66**	**0.58**	0.556	1	0.79	32.3	6.78	25.6	3.88	0.0104
06PA69	-49.6374	-74.3010	1	**32.65**	**0.82**	0.596	1	0.94	32.5	12.8	49.5	3.95	0.0565
06PA69r1	-49.6374	-74.3010	1	**22.37**	**2.12**	0.599	1	0.84	34.8	5.80	26.2	4.63	0.0170
06PA70	-49.9959	-74.0922	1	**12.08**	**0.24**	0.772	1	5.10	57.8	100	9.35	0.0955	0.5902
06PA70r1	-49.9959	-74.0922	1	**18.19**	**0.78**	0.747	1	3.37	52.5	133	2.95	0.0227	0.7433
06PA71	-49.9735	-74.1852	1	**11.67**	**0.23**	0.806	1	7.90	67.0	8.57	4.03	0.482	0.0866
06PA71r1	-49.9735	-74.1852	1	**14.81**	**0.53**	0.729	1	3.69	47.8	26.9	34.0	1.30	0.1698
06PA72	-49.9406	-74.2222	1	**16.69**	**0.34**	0.723	1	3.38	59.5	14.2	26.1	1.88	0.1020
06PA73	-49.9327	-74.3008	1	**20.35**	**0.55**	0.596	1	0.89	32.0	9.37	21.9	2.40	0.0194
06PA73r1	-49.9327	-74.3008	1	**21.02**	**2.04**	0.654	1	1.47	38.5	9.77	23.1	2.43	0.0378
06PA74	-49.9536	-74.3413	1	**16.50**	**0.31**	0.682	1	1.75	39.5	47.5	56.4	1.22	0.1455
06PA74r1	-49.9536	-74.3413	1	**18.46**	**2.15**	0.626	1	1.25	34.5	12.8	30.5	2.44	0.0356
06PA75	-50.6236	-73.7019	1	**4.90**	**0.10**	0.764	1	5.22	58.0	5.90	11.2	1.95	0.0207
06PA75r1	-50.6236	-73.7019	1	**5.87**	**1.06**	0.702	1	2.23	48.5	10.5	41.9	4.09	0.0230
06PA76	-50.9566	-73.7317	1	**13.39**	**0.23**	0.675	1	1.53	40.0	54.2	115	2.18	0.1370
06PA76r1	-50.9566	-73.7317	1	**9.97**	**6.69**	0.720	1	2.35	50.8	1.42	1.51	1.09	0.0037

Supplementary Table 2: New apatite (U-Th)/He data

Sample	Latitude	Longitude	Elevation (m)	Corrected Age (Ma)	±2σ (Ma)	Ft	No of Grains	mass (μg)	mwar (μm)	U (ppm)	Th (ppm)	Th/U	He (ncc)
anita 2	-47.1292	-72.8644	100	**8.83**	**0.30**	0.655	1	1.46	36.3	9.59	17.8	1.90	0.0147
anita 2r1	-47.1292	-72.8644	100	**12.03**	**2.12**	0.670	1	1.55	40.5	9.93	12.5	1.29	0.0202
THC2	-47.7777	-74.3182	0	**6.10**	**0.42**	0.729	2	2.93	51.5	2.38	4.18	1.76	0.0053
THC3	-47.9387	-74.8278	0	**11.57**	**0.69**	0.714	4	11.63	48.0	27.1	96.3	3.55	0.5801
THC4	-47.9413	-74.8422	0	**15.42**	**0.27**	0.670	6	9.72	40.3	90.9	113	1.25	1.4290
THC4r1	-47.9413	-74.8422	0	**16.99**	**0.44**	0.630	1	5.62	35.7	72.4	103	1.46	0.7039
THC4r2	-47.9413	-74.8422	0	**14.90**	**0.35**	0.702	5	11.25	44.5	63.9	67.6	1.08	1.1388
THC5	-47.9307	-74.7847	0	**11.03**	**0.21**	0.700	5	12.31	45.9	2.52	9.11	3.61	0.0538
THC6	-47.9780	-74.6737	0	**10.28**	**0.18**	0.669	3	5.31	43.3	19.1	56.1	2.94	0.1431
THC7	-47.9050	-74.3355	0	**9.18**	**0.32**	0.811	1	8.46	69.3	39.9	25.6	0.658	0.3505
THC7r1	-47.9050	-74.3355	0	**9.17**	**0.22**	0.750	5	15.65	48.2	52.2	56.0	1.10	0.8553
THC8	-48.0067	-74.2080	0	**5.23**	**0.90**	0.619	1	1.60	33.3	7.28	36.7	5.17	0.0101
THC8r1	-48.0067	-74.2080	0	**6.43**	**0.15**	0.715	5	18.72	48.8	7.77	36.5	4.82	0.1736
THC11	-48.1260	-73.4493	0	**5.80**	**0.31**	0.746	1	4.22	54.0	8.33	21.3	2.63	0.0302
THC11r1	-48.1260	-73.4493	0	**5.07**	**0.19**	0.610	5	5.24	34.4	12.4	24.7	2.05	0.0363
THC14	-47.5925	-72.8515	20	**3.82**	**0.06**	0.732	6	23.71	50.7	16.7	47.6	2.84	0.2247
THC16	-47.4363	-72.5880	300	**7.05**	**2.67**	0.626	1	1.36	34.0	2.25	14.1	6.42	0.0044
THC16r1	-47.4363	-72.5880	300	**7.23**	**0.22**	0.698	5	11.36	43.1	4.21	12.1	2.96	0.0513
THC17	-47.0530	-72.2478	370	**7.76**	**0.17**	0.731	2	5.91	54.4	5.31	15.7	2.95	0.0366
THC18	-47.2230	-72.6153	250	**46.47**	**2.04**	0.692	1	2.93	41.3	4.41	21.8	5.08	0.1127
THC21	-46.6288	-72.3587	380	**3.32**	**0.25**	0.711	1	2.83	45.5	13.6	63.0	4.75	0.0233
THC21r2	-46.6288	-72.3587	380	**2.32**	**0.06**	0.627	1	3.87	34.1	16.1	65.1	4.04	0.0217
THC22	-46.9065	-72.7892	330	**11.62**	**2.32**	0.645	1	1.58	35.5	10.9	17.8	1.67	0.0222
THC22r1	-46.9065	-72.7892	330	**6.89**	**0.55**	0.643	1	1.09	38.8	8.48	11.8	1.39	0.0067
THC23	-46.5187	-72.9953	200	**6.16**	**1.03**	0.571	1	0.83	28.8	56.3	112	2.04	0.0294
THC23r2	-46.5187	-72.9953	200	**4.59**	**0.09**	0.688	1	7.06	43.6	67.0	94.6	1.41	0.2414
THC24	-46.5162	-72.7292	280	**13.08**	**0.89**	0.682	1	1.70	40.5	10.8	20.3	1.92	0.0298
THC25	-46.3007	-72.7980	300	**2.57**	**0.63**	0.676	1	1.53	39.3	36.0	44.3	1.26	0.0150
THC25r1	-46.3007	-72.7980	300	**11.61**	**0.53**	0.776	5	23.20	54.3	30.9	64.7	2.15	1.1749
THC35	-44.6510	-71.7750	500	**26.13**	**0.45**	0.707	2	4.02	49.0	67.2	76.8	1.14	0.7669
THC46	-44.3723	-72.5737	10	**0.36**	**0.01**	0.702	6	14.62	44.6	58.9	104	1.77	0.0377
THC56	-43.4352	-72.1945	50	**2.56**	**0.25**	0.616	1	1.37	35.3	52.9	103	2.00	0.0201
THC56r1	-43.4352	-72.1945	50	**5.97**	**0.20**	0.676	5	7.94	38.4	58.8	85.8	1.50	0.3069
THC56r2	-43.4352	-72.1945	50	**1.48**	**0.05**	0.701	1	3.73	47.7	46.2	75.9	1.64	0.0302
THC61	-43.1760	-72.4307	30	**19.71**	**0.63**	0.695	5	15.34	62.3	24.7	14.7	0.611	0.7169
THC62	-43.1812	-71.7795	300	**22.93**	**0.92**	0.612	5	7.85	38.2	16.9	31.8	1.93	0.3276
THC64	-43.3993	-72.0930	100	**4.13**	**0.27**	0.703	1	3.00	47.0	33.3	34.4	1.06	0.0443
THC64r1	-43.3993	-72.0930	100	**5.75**	**0.18**	0.684	1	4.30	47.2	5.52	39.2	7.10	0.0310
THC65	-43.4913	-72.1087	40	**3.37**	**0.49**	0.602	1	1.42	33.8	30.7	132	4.41	0.0219
THC65r1	-43.4913	-72.1087	40	**4.94**	**0.23**	0.723	5	12.98	45.3	17.9	88.8	5.09	0.2219
THC67	-45.2968	-72.3335	100	**5.90**	**1.07**	0.666	1	1.38	48.8	11.2	69.3	6.32	0.0184
THC72	-50.2382	-74.0100	0	**11.78**	**0.46**	0.650	1	2.23	33.8	66.6	46.9	0.722	0.1614
THC72r1	-50.2382	-74.0100	0	**17.74**	**0.52**	0.722	5	13.62	43.6	51.3	29.2	0.584	1.2304
THC73	-50.1990	-74.1668	0	**22.88**	**3.35**	0.585	1	1.14	31.0	6.20	10.6	1.76	0.0164
THC73r1	-50.1990	-74.1668	0	**17.39**	**0.57**	0.713	5	13.14	42.1	8.91	20.0	2.30	0.2741
THC74	-50.0890	-74.2427	0	**17.88**	**3.70**	0.600	1	1.15	30.0	10.2	10.9	1.10	0.0190
THC74r1	-50.0890	-74.2427	0	**29.23**	**1.06**	0.634	5	6.47	41.4	10.7	6.29	0.601	0.1779
THC74r2	-50.0890	-74.2427	0	**21.06**	**1.75**	0.611	1	2.50	33.7	14.3	10.7	0.746	0.0659
THC75	-50.0300	-74.3328	0	**18.67**	**1.00**	0.652	1	1.25	36.3	32.4	0.632	0.0200	0.0602
THC75r1	-50.0300	-74.3328	0	**22.00**	**0.61**	0.821	5	18.35	58.1	19.6	2.32	0.122	0.8095
THC77	-49.9888	-74.3620	0	**15.04**	**0.60**	0.617	1	1.05	34.5	91.3	238	2.67	0.1749
THC77r1	-49.9888	-74.3620	0	**17.49**	**0.47**	0.592	5	4.83	35.8	77.9	276	3.64	0.8672
THC78	-49.9860	-74.3565	0	**28.87**	**2.15**	0.610	1	1.14	33.0	9.67	31.3	3.32	0.0423
THC78r1	-49.9860	-74.3565	0	**15.08**	**0.57**	0.690	1	3.23	47.3	5.71	14.5	2.54	0.0383
THC79	-49.8993	-74.6097	0	**11.75**	**0.72**	0.706	1	2.62	46.0	26.4	69.2	2.69	0.1131
THC79r1	-49.8993	-74.6097	0	**16.20**	**0.48**	0.673	5	8.05	39.1	46.0	99.5	2.22	0.7404
THC80	-49.8765	-74.6158	0	**12.22**	**0.96**	0.646	1	1.64	39.8	40.8	60.1	1.51	0.0865
THC80r1	-49.8765	-74.6158	0	**14.10**	**0.40**	0.654	5	8.25	38.5	45.5	81.9	1.85	0.5983

Supplementary Table 2: New apatite (U-Th)/He data

Sample	Latitude	Longitude	Elevation (m)	Corrected Age (Ma)	±2σ (Ma)	Ft	No of Grains	mass (μg)	mwar (μm)	U (ppm)	Th (ppm)	Th/U	He (ncc)
THC81	-49.9392	-74.5548	0	**15.20**	**0.75**	0.668	1	1.78	38.8	37.0	51.0	1.41	0.1075
THC81r1	-49.9392	-74.5548	0	**25.19**	**0.63**	0.709	5	12.70	47.7	11.5	39.8	3.55	0.5774
THC81r2	-49.9392	-74.5548	0	**10.81**	**0.32**	0.716	1	6.33	48.8	21.1	35.1	1.67	0.1746
THC85	-49.8453	-74.8127	0	**19.26**	**1.34**	0.539	1	0.67	28.3	33.6	30.4	0.927	0.0342
THC85r1	-49.8453	-74.8127	0	**13.53**	**0.83**	0.501	1	1.30	24.7	21.0	16.3	0.777	0.0266
THC86	-49.8517	-74.8032	0	**13.85**	**1.57**	0.670	1	1.60	40.0	12.5	15.0	1.23	0.0293
THC86r1	-49.8517	-74.8032	0	**17.92**	**1.20**	0.579	1	0.54	30.5	19.0	30.4	1.60	0.0178
THC89	-49.6050	-75.3790	100	**34.86**	**2.18**	0.594	1	0.87	31.0	24.9	32.7	1.34	0.0719
THC89r1	-49.6050	-75.3790	100	**31.88**	**1.08**	0.650	5	6.83	35.8	19.4	36.3	1.92	0.4829
THC90	-49.5932	-75.3710	0	**25.59**	**1.75**	0.661	1	1.52	39.0	11.7	66.5	5.85	0.0853
THC90r1	-49.5932	-75.3710	0	**16.77**	**0.44**	0.676	1	1.54	40.8	130	368	2.82	0.4606
THC93	-49.7135	-75.2120	0	**25.01**	**0.81**	0.627	5	6.64	37.6	49.4	28.7	0.596	0.7090
THC93r1	-49.7135	-75.2120	0	**40.24**	**1.21**	0.357	1	0.35	17.8	389	273	0.702	0.2732
THC95	-50.7883	-74.4238	0	**14.40**	**1.29**	0.616	1	1.11	33.5	26.9	59.5	2.27	0.0490
THC95r1	-50.7883	-74.4238	0	**20.15**	**0.61**	0.670	5	8.95	41.7	35.3	49.6	1.44	0.6898
THC105	-48.6885	-74.5535	0	**15.58**	**0.65**	0.627	5	7.14	39.3	16.0	17.1	0.596	0.7090
THC105r1	-48.6885	-74.5535	0	**10.49**	**0.66**	0.357	1	3.30	39.4	8.98	19.4	2.16	0.2732
THC106	-48.6167	-74.8240	0	**9.86**	**1.02**	0.667	1	1.21	42.0	12.9	46.7	3.71	0.0231
THC106r1	-48.6167	-74.8240	0	**11.69**	**0.27**	0.638	5	6.14	38.0	12.7	46.3	3.76	0.1312
THC107	-48.5767	-74.9550	0	**20.54**	**1.03**	0.531	1	0.62	25.8	60.8	123	2.08	0.0745
THC107r1	-48.5767	-74.9550	0	**16.64**	**0.39**	0.713	5	5.84	40.1	20.6	28.6	1.42	0.2310
THC108	-48.5943	-75.0037	0	**18.56**	**0.49**	0.618	5	6.30	35.6	44.3	65.4	1.51	0.5242
THC108r1	-48.5943	-75.0037	0	**17.98**	**0.41**	0.690	5	5.25	40.1	54.7	82.9	1.55	0.5857
THC109	-48.8025	-75.4655	0	**35.36**	**2.68**	0.589	1	0.90	29.8	8.15	7.49	0.943	0.0226
THC109r1	-48.8025	-75.4655	0	**17.92**	**0.44**	0.686	5	7.36	42.9	79.1	42.2	0.547	0.9789
THC110	-48.8018	-75.4427	0	**20.46**	**1.22**	0.593	1	1.06	30.8	21.1	59.8	2.91	0.0550
THC110r1	-48.8018	-75.4427	0	**16.80**	**0.37**	0.694	5	13.20	46.2	21.6	50.0	2.38	0.6266
THC111	-48.7695	-75.2022	0	**24.08**	**0.52**	0.605	5	5.76	34.9	23.7	45.6	1.98	0.3535
THC111r1	-48.7695	-75.2022	0	**20.05**	**0.45**	0.633	5	5.69	34.1	32.0	54.3	1.74	0.3957
THC112	-48.8340	-75.0518	0	**21.10**	**0.98**	0.596	1	1.59	31.3	14.8	45.2	3.12	0.0623
THC112r1	-48.8340	-75.0518	0	**20.26**	**0.49**	0.604	5	3.80	33.7	34.8	39.9	1.17	0.2507
THC114	-48.7288	-73.9872	0	**6.21**	**0.93**	0.615	1	1.38	35.0	14.2	29.3	2.12	0.0136
THC114r1	-48.7288	-73.9872	0	**6.93**	**0.17**	0.657	5	13.11	41.0	11.9	21.4	1.85	0.1238
THC115	-48.7278	-74.0458	0	**13.19**	**0.32**	0.723	5	13.01	53.7	32.5	5.58	0.176	0.5089
THC115r1	-48.7278	-74.0458	0	**15.42**	**0.38**	0.663	5	9.91	46.3	40.8	18.8	0.473	0.5554
THC116	-48.7092	-74.3288	0	**11.10**	**0.55**	0.742	1	5.02	56.8	8.48	20.9	2.53	0.0685
THC116r1	-48.7092	-74.3288	0	**10.61**	**0.24**	0.722	5	12.05	44.1	10.7	24.0	2.30	0.1871
THC117	-50.8458	-73.9458	0	**11.41**	**1.00**	0.564	1	0.99	29.8	39.0	101	2.66	0.0487
THC117r1	-50.8458	-73.9458	0	**7.68**	**0.17**	0.633	5	7.73	36.5	35.7	84.0	2.41	0.2533
THC119	-50.7933	-73.8808	0	**8.45**	**0.20**	0.631	5	4.51	38.7	20.9	27.3	1.35	0.0799
THC122	-50.5088	-73.7158	0	**6.64**	**0.43**	0.689	1	2.53	42.3	19.1	60.9	3.28	0.0468
THC122r1	-50.5088	-73.7158	0	**3.92**	**0.09**	0.682	5	13.30	40.2	10.6	25.7	2.49	0.0720
THC123	-50.5892	-73.7520	0	**5.03**	**0.20**	0.616	2	1.96	34.4	10.9	22.6	2.07	0.0119
THC124	-50.7817	-74.2575	0	**16.43**	**0.92**	0.693	1	3.10	45.8	7.28	22.0	3.10	0.0541
THC124r1	-50.7817	-74.2575	0	**10.79**	**0.24**	0.569	5	6.95	38.0	21.8	46.3	2.18	0.1704
THC141	-45.9887	-71.9090	811	**47.40**	**0.82**	0.646	3	3.96	40.0	4.79	24.8	5.18	0.1565
THC142	-45.3535	-72.4572	89	**5.65**	**0.11**	0.614	5	5.79	34.6	11.2	58.0	5.20	0.0604
FO02-07	-53.1567	-73.2935	0	**10.09**	**0.25**	0.689	1	2.15	43.75	34.8	109	3.21	0.1098
FO02-11	-52.9752	-72.9528	0	**7.01**	**0.25**	0.598	1	1.38	33.25	21.9	89.1	4.18	0.0304
FO02-18	-52.7265	-73.3678	0	**7.40**	**0.61**	0.651	1	1.71	39.25	9.90	8.93	0.925	0.0120
FO02-18r1	-52.7265	-73.3678	0	**9.35**	**0.33**	0.823	1	20.49	76.75	7.28	11.7	1.65	0.1927
FO03-26	-52.4175	-73.7598	0	**10.86**	**0.91**	0.536	1	0.76	27.50	12.5	23.3	1.92	0.0098
FO03-26r1	-52.4175	-73.7598	0	**11.30**	**1.08**	0.624	1	1.30	38.00	16.6	26.5	1.64	0.0259
FO03-26r2	-52.4175	-73.7598	0	**10.63**	**0.36**	0.665	3	5.24	40.53	9.65	20.6	2.19	0.0665
FO03-27	-52.4250	-73.7497	0	**11.13**	**1.88**	0.521	1	0.41	25.25	8.44	16.1	1.95	0.0036
FO03-28	-52.4110	-73.7437	0	**17.00**	**1.30**	0.691	1	2.26	40.50	4.93	8.81	1.84	0.0227
FO03-31	-53.3450	-73.1035	0	**7.71**	**0.57**	0.560	1	1.07	27.00	17.1	10.3	0.618	0.0110
FO03-31r1	-53.3450	-73.1035	0	**12.65**	**0.42**	0.635	5	6.31	34.67	6.83	6.10	0.916	0.0513

Supplementary Table 2: New apatite (U-Th)/He data

Sample	Latitude	Longitude	Elevation (m)	Corrected Age (Ma)	±2σ (Ma)	Ft	No of Grains	mass (μg)	mwar (μm)	U (ppm)	Th (ppm)	Th/U	He (ncc)
FO03-31r2	-53.3450	-73.1035	0	**20.03**	**2.07**	0.599	1	1.25	30.50	6.19	13.9	2.31	0.0175
FO03-32	-53.4297	-72.9127	0	**11.17**	**0.62**	0.707	1	2.96	43.50	5.59	6.86	1.26	0.0208
FO03-32r1	-53.4297	-72.9127	0	**15.30**	**3.08**	0.612	1	1.23	32.25	3.73	8.79	2.42	0.0082
FO03-33	-53.5700	-72.4032	0	**7.66**	**0.43**	0.612	1	1.41	34.00	9.25	18.5	2.05	0.0110
FO03-33r1	-53.5700	-72.4032	0	**10.69**	**1.83**	0.590	1	1.24	32.25	6.60	20.4	3.18	0.0110
FO03-33r2	-53.5700	-72.4032	0	**9.75**	**1.16**	0.643	1	2.27	36.00	6.17	14.3	2.38	0.0167
FO03-45	-53.4205	-72.5938	0	**11.94**	**0.65**	0.665	1	1.71	39.75	5.13	13.4	2.68	0.0139
FO03-50	-53.5327	-72.3527	0	**6.29**	**0.73**	0.622	1	1.54	32.25	9.88	17.7	1.84	0.0104
FO03-50r1	-53.5327	-72.3527	0	**8.17**	**1.28**	0.699	1	2.23	43.00	5.15	13.3	2.64	0.0130
FO03-50r2	-53.5327	-72.3527	0	**10.61**	**1.18**	0.667	1	2.80	39.25	5.76	13.8	2.46	0.0219
FO03-51	-53.5093	-72.5588	0	**12.14**	**0.58**	0.608	1	1.18	36.75	19.6	52.9	2.77	0.0338
FO03-51r1	-53.5093	-72.5588	0	**14.52**	**0.77**	0.677	1	2.64	43.75	12.6	48.8	3.98	0.0761
FO06-14	-55.9759	-67.2893	0	**42.43**	**3.74**	0.452	1	0.30	21.00	16.9	8.96	0.545	0.0132

Notes: mwar = mean weighted average radius; Ft = Alpha ejection correction (see main text ref. 19)

Supplementary Table 3: Compilation table of our new, as well as previously published apatite fission track data used in Figures 1, 3, and 4. Latitude and Longitude based on WGS84 geoid.

Published Apatite Fission Track Data

Latitude	Longitude	Number	Elevation	Age (Ma)	Error (1σ)
-37.1683	-72.9541	01-50	50	103.0	6.5
-37.2572	-72.9600	00-83	200	78.2	4.4
-37.3823	-71.4898	LOF143	1000	7.8	0.7
-37.3980	-73.0590	00-79	700	70.8	4.9
-37.6180	-73.1287	00-77	900	64.2	4.2
-37.7425	-73.1372	00-32	600	54.6	4.1
-37.7573	-73.1533	00-31	600	69.5	4.7
-38.0242	-73.1370	01-40	162	76.0	6.4
-38.0935	-71.7081	LOF145	850	3.9	0.7
-38.1635	-72.8965	01-35	74	99.5	6.0
-38.2301	-73.4682	Val26	0	106.0	29.0
-38.3433	-73.4867	01-04	0	89.3	7.3
-38.5535	-71.2795	LOF171	1270	34.3	4.6
-38.5960	-71.4385	LOF149	1350	40.5	6.2
-38.7628	-71.5982	WS2	-1	5.3	0.9
-39.0444	-71.8023	LOF135	370	4.2	1.2
-39.1679	-71.7257	LOF132	770	5.7	0.8
-39.4920	-72.1099	LOF131	210	16.4	1.0
-39.6756	-73.3556	Val11	10	66.3	7.6
-39.6885	-73.3471	Val10	370	53.6	5.4
-39.6971	-71.9041	LOF10	300	2.2	0.4
-39.7164	-71.8024	LOF12	1720	3.5	0.4
-39.7166	-71.8026	LOF13	1600	2.1	0.3
-39.7168	-71.8028	LOF14	1220	2.1	0.3
-39.7676	-71.8335	LOF17	1050	3.0	0.5
-39.7763	-71.6956	LOF78	1000	1.2	0.2
-39.8097	-71.5824	LOF18	1000	1.3	0.2
-39.8245	-71.9165	LOF130	290	2.8	0.5
-39.9029	-73.4979	Val14	30	55.6	6.6
-39.9572	-73.6006	Val17	0	69.7	6.2
-40.5836	-73.7390	Val42	0	39.7	3.2
-40.8533	-72.0817	AL112	850	10.6	1.3
-41.0738	-72.1242	AA130	5	6.1	0.8
-41.0925	-72.1842	AA132	10	7.2	1.8
-41.1058	-72.2752	AA129	5	4.4	0.6
-41.1427	-72.4550	AA102	50	7.1	2.3
-41.1480	-72.0718	AA131	20	6.9	1.3
-41.2069	-72.6711	AA1	80	24.9	4.7
-41.3336	-72.3631	AA35	150	6.2	0.8
-41.3633	-72.2872	AA2	30	4.4	0.5
-41.3967	-72.0633	AL122	1600	6.7	1.6
-41.4042	-72.6286	AA21	250	11.4	1.5
-41.4247	-72.5628	AA22	300	10.9	1.1
-41.4467	-72.6217	AA20	200	11.1	1.8
-41.4486	-72.2992	AA11	150	3.3	1.2
-41.4594	-72.2369	AA29	150	5.5	0.9
-41.4858	-72.3856	AA13	300	4.8	0.8
-41.4878	-72.3856	AA12	180	4.0	1.3
-41.5217	-72.3236	AA3	60	5.6	2.0
-41.5547	-72.7083	AA25	20	12.5	1.6

-41.5672	-72.3003	AA9	110	3.5	0.7
-41.5717	-72.4200	AL137	1200	9.8	1.9
-41.5769	-72.5378	AA36	200	8.2	1.3
-41.5919	-72.6769	AA24	10	9.4	2.0
-41.5919	-72.6769	AA26	10	7.8	0.9
-41.5936	-72.5786	AA23	450	8.0	1.0
-41.5997	-72.2933	AA8	80	3.3	0.6
-41.6233	-72.3572	AA4	20	3.8	0.9
-41.6283	-72.2878	AA30	100	4.0	0.9
-41.6544	-72.2658	AA31	250	4.0	0.9
-41.6753	-72.0100	AA27	200	9.3	0.8
-41.6783	-72.3819	AA34	30	4.2	0.5
-41.7250	-72.5561	AA33	20	5.8	0.5
-41.7317	-72.5494	AA37	30	7.0	1.7
-41.8004	-74.0239	Val48	-1	26.3	2.8
-41.8650	-72.2300	AL152	1550	6.7	1.7
-41.8919	-72.3950	AA42	200	4.2	2.7
-41.9487	-72.3847	AA125	100	6.5	1.2
-41.9933	-72.5794	AA43	100	16.6	2.7
-42.0056	-72.3964	AA39	150	5.7	1.9
-42.0163	-72.4618	AA106	5	4.3	1.5
-42.0305	-72.4940	AA111	5	4.7	1.2
-42.0714	-72.4722	AA45	5	4.7	1.2
-42.1294	-72.3769	AA40	40	4.3	0.7
-42.1611	-72.4583	AA44	10	3.3	0.5
-42.1708	-72.3712	AA119	5	4.9	1.7
-42.3235	-73.8410	AK614	100	77.0	18.6
-42.3355	-73.8065	AK617	20	49.9	15.7
-42.3627	-73.9213	AK611	400	78.8	31.7
-42.3782	-73.8097	AK619	20	122.2	34.7
-42.3805	-73.9890	AK621	750	81.7	21.9
-42.3839	-73.9086	LH539	200	67.6	7.5
-42.4639	-72.4203	AA32	300	3.4	1.4
-42.5380	-73.8822	AK610	350	91.5	28.3
-42.7590	-72.6070	THC58	120	4.6	1.1
-42.9098	-72.7183	THC59	5	5.0	0.9
-43.0128	-72.4712	THC60	120	1.6	1.2
-43.3500	-70.8833	CHFT163	600	69.8	14.2
-43.3500	-71.0000	CHFT168	600	67.6	10.7
-43.3993	-72.0930	THC64	100	4.9	0.8
-43.4352	-72.1945	THC56	50	5.0	0.7
-43.4913	-72.1087	THC65	40	6.0	1.0
-43.6172	-72.0072	THC66	100	6.1	1.2
-43.9693	-72.3803	THC49	50	5.6	0.8
-43.9752	-72.4690	THC54	50	1.9	0.4
-43.9893	-72.2342	THC50	100	3.0	1.1
-44.0318	-72.5513	THC55	30	3.1	0.8
-44.1678	-72.1228	THC51	270	7.2	0.9
-44.3723	-72.5737	THC46	10	1.0	0.3
-44.4452	-72.5948	THC45	5	1.4	0.6
-44.5702	-72.4402	THC43	40	4.5	1.3
-44.5825	-71.5545	THC36	600	33.1	2.8
-44.6510	-71.7750	THC35	500	86.3	4.3
-44.6935	-72.5185	THC42	50	1.9	0.7
-44.6957	-72.2417	THC38	200	15.8	3.0

-44.7277	-72.1290	THC34	250	6.9	1.9
-44.7378	-72.6875	THC40	5	3.1	0.9
-44.8535	-72.2193	THC33	300	6.5	1.0
-45.0477	-72.1042	THC32	280	5.3	0.6
-45.2292	-72.6295	THC70	50	5.4	0.5
-45.2960	-72.7448	THC69	15	4.7	0.6
-45.3205	-72.7197	THC68	30	3.7	0.9
-45.4167	-74.1667	CE9519	0	29.6	3.8
-45.4553	-72.8022	THC31	10	4.8	0.5
-45.4787	-72.2458	THC29	150	71.7	6.4
-45.5212	-72.6782	THC30	30	9.2	0.8
-45.6578	-72.4220	THC26	280	61.6	8.8
-46.5187	-72.9953	THC23	200	9.5	0.7
-47.0530	-72.2478	THC17	370	32.0	3.5
-47.4363	-72.5880	THC16	300	8.5	1.9
-47.5593	-72.7703	CB1960	1960	17.1	1.2
-47.5633	-72.8215	CB1410	1410	11.3	0.7
-47.5637	-72.8340	CB930	930	11.0	1.1
-47.5642	-72.8473	CB550	550	7.3	0.7
-47.5703	-72.8653	CB130	130	6.3	0.6
-47.5925	-72.8515	THC14	20	7.6	1.1
-47.7670	-74.0253	THC1	0	15.5	1.5
-47.7777	-74.3182	THC2	0	16.6	2.5
-47.9050	-74.3355	THC7	0	14.1	0.9
-47.9307	-74.7847	THC5	0	26.1	2.9
-47.9387	-74.8278	THC3	0	22.7	2.0
-47.9413	-74.8422	THC4	0	24.1	1.3
-47.9780	-74.6737	THC6	0	26.0	2.8
-47.9793	-73.1875	THC19	10	12.1	1.5
-48.0067	-74.2080	THC8	0	14.4	1.7
-48.1260	-73.4493	THC11	0	9.4	1.1
-49.7530	-74.7563	THC83	0	17.1	6.0
-49.8453	-74.8127	THC85	0	18.3	5.8
-49.8765	-74.6158	THC80	0	16.0	1.5
-49.8993	-74.6097	THC79	0	16.3	1.6
-49.9392	-74.5548	THC81	0	15.9	1.7
-49.9860	-74.3565	THC78	0	13.7	2.7
-49.9888	-74.3620	THC77	0	14.2	0.9
-50.0300	-74.3328	THC75	0	15.5	1.0
-50.0890	-74.2427	THC74	0	15.9	2.0
-50.1990	-74.1668	THC73	0	15.2	2.0
-50.2382	-74.0100	THC72	0	14.5	0.7
-50.5000	-75.2667	MD32	0	28.6	3.0
-51.3045	-74.9987	THC129	0	24.7	3.1
-51.3500	-75.0667	AL16	0	10.7	1.7
-51.3682	-75.0457	THC96	0	18.3	3.0
-51.4803	-74.5200	THC160	0	47.0	3.3
-51.4822	-75.1368	THC97	0	18.5	1.8
-54.6874	-69.3511	BP-102	0	27.2	5.8
-54.6926	-69.3508	BP-122	0	18.5	3.3
-54.7460	-69.6178	PIA-74	0	21.9	2.7
-54.7527	-69.6203	PIA-70	0	28.8	4.7
-54.7931	-70.3071	SV-72	0	17.3	2.2
-54.8551	-70.3544	SV-110	0	9.1	2.7
-54.8735	-69.5452	NB-72	0	30.8	4.1

-54.8962	-69.4631	NB-76	0	35.9	3.9
-54.9006	-69.4072	NB-88	0	29.4	4.4
-54.9208	-69.4842	SB-12	0	43.5	7.2
-54.9377	-69.4848	SB-14	0	55.8	12.1

New Apatite Fission Track Data

Latitude	Longitude	Number	Elevation	Age (Ma)	Error (1σ)
-38.4542	-71.3030	LOF169	950	11.3	1.6
-38.5994	-70.8287	LOF167	2270	66.9	8.3
-38.6542	-71.6021	06PA03	1334	11.2	1.1
-38.6559	-71.6014	06PA02	1490	12.8	2.0
-38.6676	-71.3874	LOF150	1300	35.6	3.0
-38.7067	-71.4700	LOF151	1450	14.5	1.8
-38.7166	-71.6208	LLA1	984	12.9	1.7
-38.7302	-71.5397	LLA6	1709	9.3	2.7
-38.7366	-71.5537	LLA4	1870	11.2	1.2
-38.8021	-71.2714	LOF155	1180	64.9	4.8
-38.8524	-71.5969	LOF158	550	2.0	1.1
-39.6466	-71.8134	LOF95	880	4.2	0.6
-39.7342	-71.8231	LOF64	670	2.7	1.2
-39.7344	-71.6945	LOF67	750	5.3	0.9
-39.7564	-71.8312	FO06-09	378	5.7	1.5
-39.7644	-71.7810	FO06-05	800	9.2	1.6
-39.8110	-72.9425	FO06-13	18	82.1	13.4
-39.8305	-71.8314	LOF19	1050	8.8	1.0
-41.0979	-71.4300	SP133	250	14.0	1.7
-41.3950	-72.0300	SP057	1325	3.5	1.1
-41.4083	-72.6467	SP067	250	10.2	1.5
-41.4933	-72.4150	SP06b	400	5.9	0.6
-41.5783	-71.7767	SP137	450	12.5	3.9
-41.5933	-71.6117	SP139	300	28.1	5.2
-41.7300	-72.6000	SP011	25	5.1	1.0
-41.8000	-71.8983	SP040	1675	13.0	2.2
-41.8617	-71.8883	SP041	1525	14.2	3.3
-41.9033	-71.9283	SP048	275	14.1	2.7
-41.9467	-72.3733	SP066	125	2.0	0.8
-41.9950	-72.3367	SP061	1650	3.9	0.7
-42.0267	-71.7600	SP043	1520	73.8	6.6
-42.0300	-71.5683	SP128	300	21.0	2.0
-42.0617	-72.1300	SP046	1450	3.4	0.5
-42.0717	-72.3300	SP062	1325	5.1	0.6
-42.6683	-72.5800	GCH02	225	5.5	1.0
-42.9133	-72.7125	THC135	10	5.8	1.0
-43.0817	-72.5550	SP080	1275	3.2	0.4
-43.2183	-72.1033	SP081	1725	6.7	0.9
-43.2500	-71.9333	AZ16	430	3.1	1.0
-43.3033	-71.8850	SP082	1700	28.6	0.5
-43.4350	-72.1367	SP084	100	3.9	0.7
-43.4500	-72.1717	SP083	1650	10.2	0.9
-43.5167	-72.7717	SP070	1450	6.5	1.0
-43.5483	-72.9667	SP069	650	8.5	1.7
-43.5533	-72.6950	SP071	1350	3.4	0.5
-43.6117	-72.5117	SP072	1490	3.8	0.8
-43.6533	-72.2550	SP074	1625	49.5	4.8
-43.7033	-72.0483	SP075	1670	41.5	6.9

-43.7033	-72.2800	SP111	75	3.3	1.0
-43.7083	-71.9167	SP076	1500	59.2	4.1
-43.7183	-72.2750	SP112	75	6.1	1.5
-43.7367	-72.2850	SP113	75	6.0	1.4
-43.9017	-72.8133	SP095	25	5.5	1.2
-44.0033	-72.6667	SP096	25	2.0	0.3
-44.0350	-73.6050	Pancho6	0	39.9	8.5
-44.0403	-73.6297	Pancho4	0	39.3	4.9
-44.4407	-72.5940	THC147	16	3.3	0.8
-44.4482	-72.5195	THC148	110	3.6	0.6
-44.4482	-72.5195	THC150	110	2.8	0.7
-44.4618	-72.5773	THC146	43	3.6	0.8
-44.7833	-73.3450	SP124	0	20.5	3.7
-44.9317	-72.1630	THC145	275	9.2	2.1
-45.0433	-73.7317	SP115	0	41.9	3.8
-45.0600	-73.4083	SP125	0	19.5	2.0
-45.2330	-72.2313	THC144	362	78.5	9.2
-45.2930	-72.3263	THC143	100	44.2	4.3
-45.3535	-72.4572	THC142	89	10.4	2.1
-45.6290	-72.4888	THC27	200	16.8	7.9
-45.9887	-71.9090	THC141	811	95.4	9.6
-46.0657	-72.0413	THC137	1211	85.8	15.7
-46.0823	-72.0510	THC136	1060	6.2	2.4
-46.1003	-72.0495	THC138	912	91.3	6.4
-46.1102	-72.1180	THC139	506	86.4	9.4
-46.1255	-72.1667	THC140	325	81.0	9.1
-46.7667	-75.5167	TP0137	0	3.1	1.3
-46.8000	-75.6000	TP0127	0	1.9	0.6
-46.8167	-75.6167	TP0128B	0	2.9	0.8
-48.5767	-74.9550	THC107	0	23.4	3.5
-48.5943	-75.0037	THC108	0	22.4	2.0
-48.6167	-74.8240	THC106	0	24.4	2.4
-48.6885	-74.5535	THC105	0	15.0	1.2
-48.7092	-74.3288	THC116	0	16.3	2.1
-48.7278	-74.0458	THC115	0	16.0	1.6
-48.7288	-73.9872	THC114	0	12.7	1.7
-48.7440	-74.9297	THC113	0	19.3	4.9
-48.7695	-75.2022	THC111	0	48.3	3.9
-48.8018	-75.4427	THC110	0	47.2	3.2
-48.8025	-75.4655	THC109	0	55.2	3.2
-48.8340	-75.0518	THC112	0	24.9	3.1
-49.3005	-74.0448	THC101	0	15.1	2.8
-49.3568	-74.1075	THC102	0	11.6	1.6
-49.4243	-74.3005	THC104	0	12.8	0.9
-49.5318	-73.8638	THC100	0	12.1	0.9
-49.5412	-74.1847	THC103	0	13.0	1.2
-49.5910	-75.4065	THC87	0	30.6	2.7
-49.5932	-75.3710	THC90	0	33.8	1.9
-49.5962	-75.3885	THC88	0	32.2	2.3
-49.6050	-75.3790	THC89	100	29.5	2.7
-49.7077	-75.2495	THC92	0	25.5	6.6
-49.7135	-75.2120	THC93	0	34.4	2.1
-50.3378	-75.1963	THC94	0	50.7	3.0
-50.4152	-74.5520	FO04-18	1	18.9	1.6
-50.4710	-74.1135	FO04-08	1	18.7	2.0

-50.5088	-73.7158	THC122	0	12.4	1.1
-50.5352	-73.8967	FO04-15	1	18.4	9.5
-50.5892	-73.7520	THC123	0	9.3	2.0
-50.6687	-73.7705	THC120	0	12.7	2.5
-50.6825	-73.7952	THC121	0	14.7	2.3
-50.7817	-74.2575	THC124	0	16.2	1.9
-50.7883	-74.4238	THC95	0	18.0	1.3
-50.7933	-73.8808	THC119	0	12.1	1.5
-50.8458	-73.9458	THC117	0	15.0	1.4
-51.4157	-73.1095	07BA25	10	18.8	3.5
-51.7555	-74.1802	THC131	0	19.0	2.4
-51.7860	-74.9705	THC155	0	45.6	3.7
-51.7958	-74.7703	THC154	0	47.5	3.0
-51.8632	-74.7913	THC156	50	42.1	4.4
-51.9517	-74.8327	THC157	10	64.2	5.9
-51.9720	-74.8062	THC159	10	58.1	4.5
-52.0087	-74.9220	THC158	10	67.7	4.7
-52.0415	-73.7443	THC132	0	17.0	4.4
-52.0808	-73.7175	THC133	0	26.6	14.0
-52.1008	-74.2353	THC153	0	17.4	2.5
-52.1085	-73.9033	THC151	0	15.3	1.5
-52.1452	-74.0403	THC152	0	15.0	1.8
-52.2562	-73.5897	THC134	0	10.0	2.5
-52.4110	-73.7437	FO03-28	1	18.5	2.5
-52.4175	-73.7598	FO03-26	1	18.5	2.8
-52.7265	-73.3678	FO02-18	1	19.6	2.7
-52.9752	-72.9528	FO02-11	1	19.7	2.6
-53.1567	-73.2935	FO02-07	1	18.2	3.1
-53.3450	-73.1035	FO03-31	1	18.3	3.1
-53.4297	-72.9127	FO03-32	1	19.8	3.1
-53.5327	-72.3527	FO03-50	1	18.6	3.3
-53.5700	-72.4032	FO03-33	1	19.0	3.5
-55.9759	-67.2893	FO06-14	1	100.0	10.7